

Figure 1 The Lithium-11 nucleus consists of a core Lithium-9 nucleus orbited by two neutrons. If any one of the three bodies is removed the remaining two would be unbound, rather like heraldic Borromean rings.

Borromean nuclei

1 Introduction

The nucleus ^{11}Li is a prototype of a halo nucleus with fascinating properties. The reason is its unusual large radius and the difficulty in explaining its properties by means of traditional theoretical tools. As seen in Table 3.3 the nucleus ^{10}Li is not bound, having a resonant state at ~ 500 keV in the continuum. However ^{11}Li is bound by ~ 350 keV. The valence neutrons in ^{11}Li have to be treated separately from the core nucleons in order to explain its properties (i.e., radius) with traditional techniques. Thus, it seems that ^{11}Li should be treated theoretically as a three-body problem, $^9\text{Li} + n + n$; in which to a good approximation ^9Li is treated as an inert core. This assumption is supported by the fact that the valence neutrons are distributed in a spatial region which is much larger than the core. As seen in before $r_{\text{ms}}(^{11}\text{Li}) \cong 3.1$ fm while $r_{\text{ms}}(^9\text{Li}) \cong 2.4$ fm. Calling $r_{\text{ms}}(n)$ the root mean square radius of the distribution of a valence neutron, one can write

$$r_{\text{ms}}(^{11}\text{Li}) \cong \frac{2}{11} r_{\text{ms}}(n) + \frac{9}{11} r_{\text{ms}}(^9\text{Li}) \cong \frac{2}{11} (6 \text{ fm}) + \frac{9}{11} (2.4 \text{ fm}). \quad (1)$$

Thus, the r_{ms} of the valence distribution is of order of 6 fm, which is much larger than $r_{\text{ms}}(^9\text{Li})$. In other words, the valence neutrons in ^{11}Li “see” the core (^9Li) almost like a point particle.

The properties of the three-body halo nuclei were so intriguing that a new name was coined for them by J.S. Vaagen and M. Zhukov: *Borromean nuclei* [1]. The name recalls the Borromean rings, heraldic symbol of the princes of Borromeo, which are carved in the stone of their castle on an island in Lago Maggiore in Northern Italy. The three rings are interlocked in such a way that if any of them were removed, the other two would also fall apart. The 3-body quantum analog is one where the 3-body system is bound, but where none of the two-body subsystems are bound.

Nature has realized Borromean systems in loosely bound halo-like nuclei such as ^{11}Li , which are now produced as secondary beams. To understand these systems one needs to go beyond the mean field approach, to few-body theoretical procedures such as expansion on *hyperspherical harmonics* or the coordinate space *Faddeev approach*. Nuclei like ^6He and ^{11}Li can (a realistic starting point!) be modeled as a core surrounded by two loosely bound valence neutrons. Not only the bound state (^6He and ^{11}Li both have only one bound state!), but also the structure of the continuum and the details of reaction mechanisms can be described in this way.

Besides the three-body halos (e.g., ^6He , ^{11}Li) the two-body halos (e.g., ^8Be , ^{11}Be , ^{19}C , etc.) can also be treated in terms of a core and a proton, or neutron, outside the core. Some characteristics of these nuclei can be reproduced in this way. However, to obtain the correct assignments of spin and parity and the model has to be improved.

Supplement A

2 The singlet state in the deuteron

Before we go ahead and look for the properties of ^{11}Li from the point of view of a three-body problem, let us recall some useful concepts of the two-nucleon system, in particular the deuteron.

The binding energy of the deuteron is ~ 2.2 MeV which is very small (~ 1 MeV for each nucleon) as compared with the binding energy of a nucleon in a large nucleus, which is of order of 8 MeV. It is also observed experimentally that there is no excited state of the deuteron. We have shown that these properties can be obtained by simulating the interaction of the neutron and the proton in the deuteron by a square well potential with depth $V_0 \cong 36$ MeV and a range of $r_0 \sim 2$ fm. It was also seen that the size of the deuteron is larger than the range of this potential. Beyond the range of the potential the deuteron wavefunction $u(r)/r \sim e^{-\eta r}/r$ (a Yukawa function), with $\hbar^2\eta^2/m_N = B$.

We now look for the continuum states of the n-p system. I.e., for $E > 0$. We again consider a square-well potential and $\ell = 0$. Thus

$$\frac{d^2u_i}{dr^2} + p^2u_i = 0 \quad , \quad \text{for } r \leq r_0, \quad \frac{d^2u_0}{dr^2} + k^2u_0 = 0 \quad , \quad \text{for } r > r_0 \quad (2)$$

where

$$p^2 = \frac{m_N(V_0 + E)}{\hbar^2} \quad , \quad k^2 = \frac{m_N E}{\hbar^2} . \quad (3)$$

Since $u \rightarrow 0$ as r does, the solution of 2, for $r \leq r_0$ is

$$u_i = D \sin(pr) . \quad (4)$$

Similarly, for $r > r_0$,

$$u_0 = C \sin(kr + \delta) . \quad (5)$$

Matching the logarithmic derivatives at $r = r_0$ yields

$$p \cot (p r_0) = k \cot (k r_0 + \delta). \quad (6)$$

For $E \sim 0$ we can approximate $p \cot (p r_0) \cong -\eta$ which is the logarithmic derivative of $e^{-\eta r}$. Thus,

$$p \cot (p r_0) \cong -\eta = -\frac{\sqrt{m_N B}}{\hbar} \quad (7)$$

and

$$\cot (k r_0 + \delta) \cong -\frac{\eta}{k}. \quad (8)$$

For $E \sim 0$, $k r_0 \ll 1$, $\delta \ll 1$ and $k^2 \ll \eta^2$ and the above equation becomes

$$\delta \cong -\frac{k}{\eta} - k r_0. \quad (9)$$

The scattering cross section at low energies is

$$\sigma_{sc} \cong \frac{4\pi}{k^2} \delta^2 = 4\pi \left(\frac{1}{\eta} + r_0 \right)^2. \quad (10)$$

Using $1/\eta = 4.3$ fm, $r_0 = 2$ fm, we find $\sigma_{sc} = 5$ b. Alternatively, if we neglect r_0 as compared to $1/\eta$ we find

$$\sigma_{sc} \cong \frac{4\pi}{\eta^2} = 2.3 \text{ b}. \quad (11)$$

Other approximations give values somewhere between these two ranges. The experimental value is however $\sigma_{sc} = 20.4$ b.

This bad agreement can be explained as follows. The n-p system depends very much on its spin properties. The proton and neutron have spin $1/2$ and their spin wave function is to be described by two states $\chi^{(+1/2)}$ and $\chi^{(-1/2)}$, spin-up and spin-down, respectively. The n-p system is a combination of these wave functions with

$$\xi_s = \frac{1}{\sqrt{2}} \left\{ \chi^{(+)}(p)\chi^{(-)}(n) - \chi^{(+)}(n)\chi^{(-)}(p) \right\} \quad (12)$$

$$\xi_t^{(+1)} = \chi^{(+)}(p)\chi^{(+)}(n) \quad (13)$$

$$\xi_t^{(0)} = \frac{1}{\sqrt{2}} \left[\chi^{(+)}(p)\chi^{(-)}(n) + \chi^{(+)}(n)\chi^{(-)}(p) \right] \quad (14)$$

$$\xi_t^{(-1)} = \chi^{(-)}(p)\chi^{(-)}(n) \quad (15)$$

where ξ_s and ξ_t are known as singlet and triplet states. They correspond to total spin 0 and 1, respectively. Experimentally it is found that the deuteron spin is 1. Therefore, the deuteron is in a triplet state.

When proton and neutron scatter ($E > 0$) they can be in any of the states described above. In a general scattering experiment, the spin of the nucleons are randomly oriented and the n-p system is in the triplet and singlet states in proportion to the corresponding

weight factors for these states, which are, respectively, $3/4$ and $1/4$. The total scattering cross section consists of two parts

$$\sigma = \frac{3}{4}\sigma_t + \frac{1}{4}\sigma_s \quad (16)$$

where σ_t and σ_s are the cross sections for scattering in the triplet and singlet states respectively.

Because of the preference for the triplet state for the deuteron we also assume this preference for the n-p scattering at $E \sim 0$. Following Eq. 10 we write

$$\sigma = 3\pi \left(\frac{1}{\eta_t} + r_t \right)^2 + \pi \left(\frac{1}{\eta_s} + r_s \right)^2 \quad (17)$$

where

$$\eta_t = \sqrt{\frac{m_N B}{\hbar^2}} \quad , \quad \eta_s = \sqrt{\frac{m_N E_s}{\hbar^2}}. \quad (18)$$

E_s is the energy of a singlet state, which can only exist in the continuum.

Assuming $r_t \cong r_s \cong 2$ fm, using $\sigma = 20.4$ b and $1/\eta_t = 4.3$ fm we get

$$\left| \frac{1}{\eta_s} \right| = 25 \text{ fm} \quad (19)$$

which gives $|E_s| = 66$ keV. Eqs. 17 and 18 do not determine the sign of η_s and E_s . However, the scattering length a_s is negative, if one uses the theory to fit the experimental data [2] ($a_t = 5.37$ fm, $a_s = -23.73$ fm). Hence the $E_s = 66$ keV singlet state is not a bound deuteron state, but a virtual state.

3 Two loosely-interacting particles in a potential well

The three-body ^{11}Li problem amounts to solving the Hamiltonian

$$\mathcal{H} = H_1(\mathbf{r}_1) + H_2(\mathbf{r}_2) + H'(\mathbf{r}_1, \mathbf{r}_2) \quad (20)$$

where \mathbf{r}_1 and \mathbf{r}_2 are the coordinates of the two neutrons with respect to ^9Li , assumed to be infinitely heavy.

The ground state energy of ^{11}Li would be

$$\langle \psi | \mathcal{H} | \psi \rangle = 2\epsilon_n + \langle \psi | H' | \psi \rangle \quad (21)$$

where ψ is the ground-state wavefunction. To find ψ is a big task, involving the solution of the Fadeev equations (see next Section).

However, a qualitative argument, originally presented by Migdal [3], can be given to show that, although ^{10}Li is unbound, ^{11}Li can be in a bound state. For this it is necessary that ^{10}Li has a resonant state in the continuum.

Then we can assume that the behavior of the neutron wavefunctions is dominated by the resonant state, i.e., $\psi_n \sim \psi_{n'} \sim \psi_{\text{res}}$. The energy of this state is $\epsilon_{\text{res}} \sim 500$ keV. If the radial wavefunctions are little affected by H' , then

$$\langle \psi | \mathcal{H} | \psi \rangle \cong 2\epsilon_{\text{res}} + \langle H'(\mathbf{r}_1, \mathbf{r}_2) \rangle. \quad (22)$$

To simplify the calculations, let us assume that $H'(\mathbf{r}, \mathbf{r}') = -v_0(r)\delta(\mathbf{r} - \mathbf{r}')$. Then the integral of the second term reduces to a single integral. That is,

$$\langle H' \rangle \cong \int \psi_{\text{res}}^4(r) v_0(r) d^3r. \quad (23)$$

The wavefunction $\psi_{\text{res}}(r)$ can be approximated by

$$\psi_{\text{res}}(r) = \frac{A}{\sqrt{4\pi}} \begin{cases} (\sin kr)/r & \text{for } r < R \\ \Lambda & \text{for } r > R \end{cases} \quad (24)$$

when $E \sim 0$. R is the range of the neutron+ ${}^9\text{Li}$ potential, which we assume $R \cong 3.2$ fm. Also, $\hbar k = \sqrt{2m_N(E + U_0)} \cong \sqrt{2m_N U_0}$, where $U_0 \sim 50$ MeV is the depth of the $n + {}^9\text{Li}$ potential and A is a normalization constant.

We now show that the form of the wavefunction for $r > R$ is irrelevant. The neutron-neutron interaction can be taken as

$$v_0(r) = -v_0 e^{-r^2/r_0^2} \quad (25)$$

where $v_0 \sim 50$ MeV, $r_0 \sim 2$ fm.

The integral 23 becomes

$$\begin{aligned} \langle H' \rangle &= -\frac{A^4}{4\pi} v_0 \left\{ \int_0^R \frac{\sin^4 kr}{r^2} e^{-r^2/r_0^2} dr + \Lambda^4 \int_R^\infty \frac{e^{-r^2/r_0^2}}{r^2} dr \right\} \\ &= -\frac{A^4}{4\pi} v_0 \{0.887 + 3.20 \times 10^{-3}\}, \end{aligned} \quad (26)$$

using the values given above.

It is also natural to normalize $\psi_{\text{res}}(r)$ inside the range $r < R$ since in a resonant state the particle has a larger amplitude to be found within the range of the potential. Neglecting the second term in 26 we obtain

$$\langle H' \rangle \sim -2.5 \times 10^{-2} v_0 \sim -1.25 \text{ MeV}. \quad (27)$$

Using this value in 22 we find that

$$\mathcal{E}_{\text{ground}}^{11\text{Li}} \sim -0.25 \text{ MeV}, \quad (28)$$

which is close to the experimental value.

Of course, this result is based on the assumption that the $n - n$ interaction can be considered as a perturbation, but it comes out larger than $2\epsilon_{\text{res}}$. Thus,

the conclusion is that H' is essential to produce the binding in ^{11}Li . Although the dineutron system is not bound, it can become bound in the presence of a core nucleus [3].

Based on this idea Hansen and Jonson [10] proposed that much of the properties of ^{11}Li can be obtained by assuming an inert ^9Li -core bound to a particle called by *di-neutron*. As in the case of the deuteron the wavefunction for ^{11}Li at large distances is given by $\psi_{2n-^9\text{Li}}(r) \sim e^{-\eta r/r}$, with $\eta = \sqrt{2\mu B}/\hbar \cong 6 \text{ fm}^{-1}$.

Supplement B

4 Variational methods

The Schrödinger equation

$$H|\psi\rangle = E|\psi\rangle \quad (29)$$

is equivalent to the variational equation

$$\delta E(\psi) = 0 \quad (30)$$

where

$$E(\psi) = \frac{\langle\psi|H|\psi\rangle}{\langle\psi|\psi\rangle}. \quad (31)$$

The variation is obtained by modifying the initial (normalized) wavefunction by

$$\psi' = \psi + \delta\psi. \quad (32)$$

Replacing 32 in 31, we obtain

$$\begin{aligned} E(\psi') &= \frac{\langle\psi'|H|\psi'\rangle}{\langle\psi'|\psi'\rangle} = \frac{\langle\psi + \delta\psi|H|\psi + \delta\psi\rangle}{\langle\psi'|\psi'\rangle} \\ &= E + \frac{\langle\psi|[H - E]|\psi\rangle}{\langle\psi|\psi\rangle} \end{aligned} \quad (33)$$

where in the last step we assumed $\delta\psi$ small and $\langle\delta\psi|\psi\rangle = 0$.

Hence $\delta E = E(\psi') - E = 0$ implies 29. Also, δE is quadratic in $\delta\psi$ and if E_0 is the lowest eigenvalue of H , then $(H - E_0)$ is a positive operator and $E(\psi') \geq E_0$. This observation leads to the conclusion that $E(\psi)$ must be minimized with respect to the parameters on which ψ depends in order to approximate the true lowest eigenvalue of H .

That is, for $\psi = \psi(\alpha_i)$

$$\begin{aligned}
\frac{\partial E}{\partial \alpha_i} &= \frac{1}{(\langle \psi | \psi \rangle)^2} \left\{ \langle \psi | \psi \rangle \left[\left\langle \frac{\partial \psi}{\partial \alpha_i} \middle| H | \psi \right\rangle + \langle \psi | H \middle| \frac{\partial \psi}{\partial \alpha_i} \right] - \right. \\
&\quad \left. - \langle \psi | H | \psi \rangle \left[\left\langle \frac{\partial \psi}{\partial \alpha_i} \middle| \psi \right\rangle + \langle \psi | \frac{\partial \psi}{\partial \alpha_i} \right] \right\} \\
&= \frac{1}{\langle \psi | \psi \rangle} \left\{ \left\langle \frac{\partial \psi}{\partial \alpha_i} \middle| H - E(\psi) | \psi \right\rangle + \langle \psi | H - E(\psi) \middle| \frac{\partial \psi}{\partial \alpha_i} \right\} \\
&= 0
\end{aligned} \tag{34}$$

where we have used Eq. 33.

The important step in this method is to choose a parametrized trial wavefunction ψ that reflects the main features of the interaction.

For the three-body system a trial function can be a simple product

$$\psi = \phi(r_1)\phi(r_2)\phi(r_3). \tag{35}$$

We would then be looking for the best ϕ that would lead to a stationary E .

As an illustration consider a simple attractive two-body potential

$$V(r) = -V_0 \frac{e^{-r/r_0}}{(r/r_0)}. \tag{36}$$

A possible trial wavefunction for a system of 3 identical particles is

$$\psi_1 = e^{-\alpha(r_1+r_2+r_3)} \tag{37}$$

with the non-linear parameter α that is varied to yield the lowest ground state energy. A second trial wavefunction is

$$\psi_2 = \sum_{i=1}^N a_i \widehat{S} e^{-\alpha(jr_1+kr_2+\ell r_3)} \tag{38}$$

for which the parameters $a_i, i = 1, \dots, N$ are varied while α is kept fixed. \widehat{S} is the symmetrization operator and j, k, ℓ are integers depending on the value of i .

In general, as the two-body interaction becomes more complicated by the addition of such features as the repulsive core, the tensor component, etc., the search for a satisfactory trial wavefunction becomes more involved, too.

Completely equivalent to a variational procedure is a diagonalization calculation. In this case ψ is expanded in terms of a complete set of wavefunctions ψ^ν

$$\psi = \sum_{\nu} a_{\nu} \psi^{\nu}. \tag{39}$$

The exact wavefunction for a given E is determined by diagonalizing the matrix $H_{\mu\nu} = \langle \psi^\mu | H | \psi^\nu \rangle$. For a complete set of antisymmetric ψ^ν (with $\nu \rightarrow \infty$), the diagonalization of the matrix $\langle \psi^\mu | H | \psi^\nu \rangle$ would result in a series expansion of Ψ . But taking a large

set of ψ^ν would involve a prohibitive amount of work, and generally only a few terms on the right side of Eq. 39 are retained. Actually, a few values of ν are sufficient to determine a ψ which is a good approximation to the exact wavefunction, provided the set of ψ^ν 's chosen is such that some of them are fairly close to the actual wavefunction.

5 A variational calculation for ^{11}Li

The Hamiltonian for ^{11}Li is given by

$$H = \frac{\mathbf{p}_1^2 + \mathbf{p}_2^2}{2m_N} + \frac{\mathbf{p}_3^2}{2m_9} - \frac{(\mathbf{p}_1 + \mathbf{p}_2 + \mathbf{p}_3)^2}{2(2m_N + m_9)} \\ + V_{nn}(|\mathbf{r}_1 - \mathbf{r}_2|) + V_{n-9}(|\mathbf{r}_1 - \mathbf{r}_3|) + V_{n-9}(|\mathbf{r}_2 - \mathbf{r}_3|) \quad (40)$$

where the two neutrons and ^9Li are labeled by 1,2 and 3, respectively. The center of mass kinetic energy is subtracted from Eq. 40 (3rd term on the rhs). Transforming to Jacobi coordinates the corresponding momenta are

$$\mathbf{p}_\rho = \frac{1}{2}(\mathbf{p}_1 - \mathbf{p}_2) \quad (41)$$

$$\mathbf{p}_\lambda = \frac{m_9(\mathbf{p}_1 + \mathbf{p}_2) - 2m_N\mathbf{p}_3}{m_9 + 2m_N} \quad (42)$$

$$\mathbf{R} = \frac{m_N(\mathbf{r}_1 + \mathbf{r}_2) + m_9\mathbf{r}_3}{m_9 + 2m_N}, \quad \mathbf{p}_R = \mathbf{p}_1 + \mathbf{p}_2 + \mathbf{p}_3 \quad (43)$$

so that

$$H = \frac{p_\rho^2}{m_N} + \frac{p_\lambda^2}{2\mu} + V_{nn}(\rho) \\ + V_{n9}\left(|\boldsymbol{\lambda} - \frac{1}{2}\boldsymbol{\rho}|\right) + V_{n9}\left(|\boldsymbol{\lambda} + \frac{1}{2}\boldsymbol{\rho}|\right) \quad (44)$$

where $\mu = 2m_N m_9 / m_{11}$ is the reduced mass of the ^9Li -dineutron system. The interactions depend on the absolute values of $\boldsymbol{\lambda}$ and $\boldsymbol{\rho}$ and the angle θ between their directions. The three remaining degrees of freedom correspond to relations of the entire three particle system. For the calculation of the ground-state ($S = 0$) one may neglect the rotational degrees of freedom.

Johannsen, Jensen, and Hansen [5] used the following potentials

$$V_{nn}(r) = \sum_k S_\rho^k \exp\left[-(r/b_\rho^k)^2\right] \\ V_{n9}(r) = \sum_k S_\lambda^k \exp\left[-(r/b_\lambda^k)^2\right]. \quad (45)$$

The ground state wavefunctions can be expanded in terms of harmonic oscillator wavefunctions,

$$\psi(\rho, \lambda, \theta) = (\alpha\beta)^{3/4} \sum_{n\rho\ell} a_{n\rho}^\ell R_{n\ell}(\alpha\rho^2) R_{\rho\ell}(\beta\lambda^2) \left(\ell + \frac{1}{2}\right)^{1/2} P_\ell(\cos\theta) \quad (46)$$

where P_ℓ is the ℓ th Legendre Polynomial and $R_{n\ell}$ is the properly normalized radial wavefunction. Only even ℓ -values need to be included as the Hamiltonian is even under the transformation $\theta \rightarrow \pi - \theta$ and the odd values of ℓ correspond to excited states. For a given size of the basis the precision is improved by treating also the scale parameters α and β as variational parameters, in addition to the expansion coefficients $a_{n\rho}^\ell$. The Schrödinger equation can now be solved by diagonalization to obtain the energy E_{11} .

The neutron-neutron potential is chosen so as to reproduce the low-energy scattering data, which through the known $\ell = 0$ scattering length and effective range parameter determines the two parameters of a single Gaussian uniquely: $S_\rho = -31$ MeV, $b_\rho = 1.8$ fm. This is a good approximation and no additional terms in Eq. 45 is needed.

No available data is known of scattering of neutrons on ^9Li . To construct the potential one can fold a Gaussian (or harmonic oscillator) density distribution of ^9Li with an average range of the nucleon-nucleon interaction. One obtains $b_\lambda \cong 2.4$ fm. With this value, a potential depth $S_\lambda \cong -10$ MeV corresponds to the limit of no binding of ^{10}Li . The Gaussian potentials fall off more rapidly than the correct long-range weakly attractive potential. Thus, various types of V_{ng} potentials can be tested [5].

For each set of potentials parameters a variational calculation yields

$$\begin{aligned}
 E_\rho &= \langle \psi | -\frac{\hbar^2}{m_N} \nabla_\rho^2 + V_{nn}(\rho) | \psi \rangle \\
 E_\lambda &= \langle \psi | -\frac{\hbar^2}{2\mu} \nabla_\lambda^2 + V_{n9} \left(|\lambda - \frac{1}{2} \rho| \right) + V_{n9} \left(|\lambda + \frac{1}{2} \rho| \right) | \psi \rangle \\
 \delta \langle r^2 \rangle &= \frac{1}{11} \left\{ \frac{18}{11} \langle \psi | \lambda^2 | \psi \rangle + \frac{1}{2} \langle \psi | \rho^2 | \psi \rangle \right\} \\
 \langle p_n^2 \rangle &= \langle \psi | p_\rho^2 | \psi \rangle + \frac{1}{4} \langle \psi | p_\lambda^2 | \psi \rangle
 \end{aligned} \tag{47}$$

where

$$\delta \langle r^2 \rangle \equiv \langle r^2 \rangle_{11} - \frac{9}{11} \langle r^2 \rangle_9 \tag{48}$$

represents (2/11)th of the mean-square radius of a neutron in the halo.

A set of parameters ($b_\lambda^{(1)}, S_\lambda^{(1)} = 2.0$ fm, 15 MeV and $b_\lambda^{(2)}, S_\lambda^{(2)} = 2.5$ fm, -17 MeV) was found [5] that reproduce the experimental value of $\delta \langle r^2 \rangle \cong 6$ fm and $E_{11} \cong -0.3$ MeV. One observes that the first parameters correspond to a repulsive Gaussian potential.

Contrary to the simple estimates, it was found [5] that E_ρ is always positive, for all set of parameters tested. This shows that a three body system has subtle intrinsic structure, which are in most times not obtainable from two-body arguments only.

In this model, the intrinsic (ρ) and relative (λ) coordinates have a most probable value of 3.3 fm and 3.1 fm, respectively. A sphere with radius of 2.2 fm (the

core of ^{11}Li) has a probability of 0.8 for having both neutrons outside the sphere. For comparison, a dineutron model with (normalized) wavefunction

$$\psi(r) = \frac{\eta}{2\pi} e^{-\eta r} \quad (49)$$

yields a value of $P(r > r_0) = e^{-2\eta r_0}$. Thus, the probability that both neutrons are outside the core is ~ 0.5 for the dineutron model. This value can increase somewhat if one corrects Eq. 49 for the distortion caused by a finite range potential. For a square-well potential with radius R the wavefunctions for $r > R$ can be approximated by [10]

$$\psi(r) = \sqrt{\frac{\eta}{2\pi}} \frac{e^{\eta R}}{\sqrt{1 + \eta R}} \frac{e^{-\eta r}}{r} \quad (50)$$

With this wavefunction the probability that both neutrons are at $r > R = 2.2$ fm is 0.6.

If one switches off the $n - n$ interaction (i.e., $S_\rho = 0$) it is not possible to get ^{11}Li bound and ^{10}Li unbound at the same time. Also, in this case, the most probable separation* between the neutrons is now 5.6 fm and the dineutron-core separation is 2.9 fm. Thus the $n - n$ interaction is very important in determining the properties of ^{11}Li . It also brings the neutrons closer together in the halo.

*In case one takes ^{10}Li as bound.

Supplement C

6 Two-body scattering at low energies
6.1 Partial wave decomposition

If $E > 0$, the energy of a two-body system can attain any value. For a spherically symmetric potential and for each value of E the wave equation reduces to

$$\frac{d^2 u_\ell}{dr^2} + \left\{ \frac{2\mu}{\hbar^2} [E - V(r)] - \frac{\ell(\ell+1)}{r^2} \right\} u_\ell = 0 \quad (51)$$

where

$$\psi(r) = \sum_{\ell=0}^{\infty} a_\ell(k) \frac{u_\ell(r)}{r} P_\ell(\cos \theta), \quad \text{with} \quad k = \sqrt{\frac{2\mu E}{\hbar^2}}. \quad (52)$$

For $r \rightarrow \infty$, $V(r) \rightarrow 0$ and $\ell(\ell+1)/r^2 \rightarrow 0$. The solution of Eq. 51 is

$$u_\ell(r) \sim \sin \left(kr - \frac{\ell\pi}{2} + \delta_\ell \right) \quad (53)$$

where δ_ℓ is the scattering phase shift.

The total wavefunction is composed of an incident plane wave and a scattered wave (Eq. ??)

$$\psi \cong e^{i\mathbf{k}\cdot\mathbf{r}} + f(\theta) \frac{e^{ikr}}{r}.$$

Expanding in Legendre polynomials

$$\psi(r, \theta) \cong \sum_{\ell=0}^{\infty} \left[(2\ell+1) i^\ell j_\ell(kr) + f_\ell \frac{e^{ikr}}{r} \right] P_\ell(\cos \theta) \quad (54a)$$

where

$$f(\theta) = \sum_{\ell} f_\ell P_\ell(\cos \theta) \quad (55)$$

and $j_\ell(kr)$ is the spherical Bessel function. At $r \rightarrow \infty$

$$j_\ell(kr) \longrightarrow \frac{1}{kr} \sin(kr - \ell\pi/2). \quad (56)$$

Using Eq. 53, and comparing Eq. 52 with Eq. 54a one finds

$$f(\theta) = \frac{1}{k} \sum_{\ell=0}^{\infty} (2\ell+1) e^{i\delta_\ell} \sin \delta_\ell P_\ell(\cos \theta). \quad (57)$$

The probability current is given by

$$\mathbf{S} = \frac{\hbar}{\mu} \text{Im} [\psi^* \nabla \psi]. \quad (58)$$

For the incident wave

$$S_i = \frac{\hbar}{\mu} \operatorname{Im} \left[e^{-ikz} \frac{d}{dz} e^{ikz} \right] = \frac{\hbar k}{\mu} = v. \quad (59)$$

For the scattered wave, the radial current is

$$S_r = \frac{\hbar}{m} \operatorname{Im} \left\{ f^*(\theta) \frac{e^{-ikr}}{r} \frac{\partial}{\partial r} \left[f(\theta) \frac{e^{ikr}}{r} \right] \right\} = \frac{v}{r^2} |f(\theta)|^2. \quad (60)$$

The differential scattering cross section is defined as

$$\frac{d\sigma}{d\Omega} = \frac{r^2 S_r}{S_i} = |f(\theta)|^2 = \frac{1}{k^2} \left| \sum_{\ell=0}^{\infty} (2\ell+1) e^{i\delta_\ell} \sin \delta_\ell P_\ell(\cos \theta) \right|^2. \quad (61)$$

The total cross section is

$$\sigma = \int \frac{d\sigma}{d\Omega} d\Omega = \frac{4\pi}{k^2} \sum_{\ell=0}^{\infty} (2\ell+1) \sin^2 \delta_\ell. \quad (62)$$

It is maximum whenever

$$\delta_\ell = \left(n + \frac{1}{2} \right) \pi, \quad n = 0, \pm 1, \pm 2, \dots \quad (63)$$

which is a resonance condition.

If $E \rightarrow 0$ ($k \rightarrow 0$) and V is very small, $f_\ell \rightarrow 0$, and

$$\psi(\mathbf{r}) \simeq \sum_{\ell=0}^{\infty} B_\ell(kr) P_\ell(\cos \theta)$$

where

$$B_\ell(kr) = (2\ell+1) i^\ell j_\ell(kr),$$

i.e.,

$$\begin{aligned} B_0(kr) &= \frac{\sin(kr)}{kr} \simeq 1 - \frac{(kr)^2}{6} + \dots \\ B_1(kr) &= i3 \left[\frac{\sin(kr)}{(kr)^2} - \frac{\cos(kr)}{kr} \right] \\ &\simeq i \left[kr - \frac{(kr)^3}{10} + \dots \right] \end{aligned} \quad (64)$$

Thus, at $r \sim r_0$,

$$\left| \frac{B_1}{B_0} \right|^2 \simeq (kr_0)^2 \quad (65)$$

For a neutron-proton system scattering at 1 MeV in the laboratory system, and using $r_0 \sim 2$ fm, only 9% of the scattering is due to $\ell = 1$. In fact, for laboratory energies up to 10 MeV, s -scattering ($\ell = 0$) is predominant.

In the absence of a potential, and $\ell = 0$

$$\psi_{\ell=0} \sim \frac{\sin(kr)}{kr} = \frac{e^{ikr} - e^{-ikr}}{2ikr}. \quad (66)$$

In the presence of a potential, Eq. 53 yields

$$\psi_{\ell=0}^{(r)} = \frac{u_{\ell=0}(r)}{r} \xrightarrow{r \rightarrow \infty} \frac{\sin(kr + \delta_0)}{r} \sim \frac{e^{i(kr+2\delta_0)} - e^{-ikr}}{2ikr}, \quad (67)$$

since this is a mere proportionality.

The difference between Eq. 67 and Eq. 66 is the scattered wave

$$\psi_{sc} \sim \frac{e^{ikr}}{2ikr} \left(e^{2i\delta_0} - 1 \right). \quad (68)$$

For elastic scattering, δ_0 is real, and the probability currents are

$$|\text{ingoing wave}| = |\text{outgoing wave}|.$$

Also, for $\ell = 0$, the total scattering cross section is

$$\sigma_{sc} = \frac{4\pi}{k^2} \sin^2 \delta_0 \quad (69)$$

which is angle-independent.

6.2 Scattering length

For $E \rightarrow 0$, and $\ell = 0$ (unnormalized!),

$$u = r\psi = e^{i\delta} \frac{\sin(kr + \delta)}{k} \quad (70)$$

where $\delta \equiv \delta_0$. If u is finite, δ must approach zero as k does. Defining

$$a = \lim_{k \rightarrow 0} \left(-\frac{\sin \delta}{k} \right) \quad (71)$$

we get from Eq. 69

$$\sigma_{sc} = 4\pi a^2. \quad (72)$$

Thus a has the significance of the radius of a hard sphere from which the scattering occurs (note that classically $\sigma_{sc} = \pi a^2$).

Eq. 71 also means $\delta/k = -a$, and we can rewrite 70 as

$$\lim_{k \rightarrow 0} u \sim \frac{kr}{k} + \frac{\delta}{k} = r - a. \quad (73)$$

Thus, the scattering length a is the intercept of u on the r -axis (see Fig. 2.

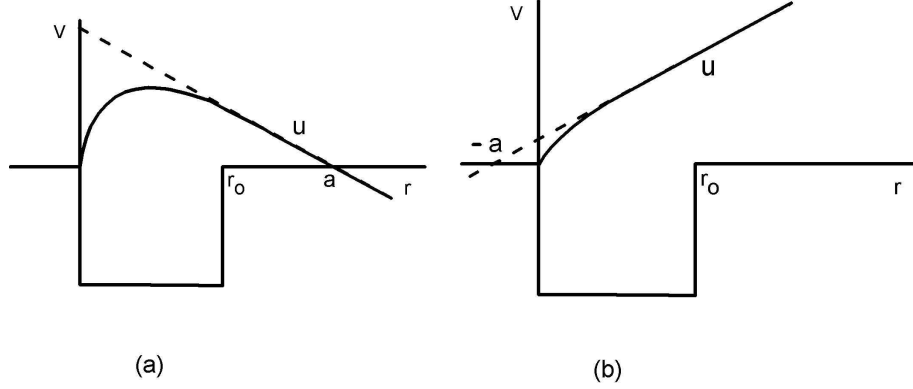


Figure 2 A scattering state with (a) positive and (b) negative scattering length.

6.3 Effective range theory

The energy dependence of σ_{sc} can be expressed in terms of the scattering length and another parameter which is called *effective range*. We will denote it by r_0 .

For $E = \hbar^2 k^2 / 2\mu$ and $E = 0$,

$$u'' + \left(k^2 - \frac{2\mu V}{\hbar^2}\right) u = 0, \quad \text{and} \quad u_0'' - \frac{2\mu V}{\hbar^2} u_0 = 0. \quad (74)$$

Multiplying by u_0 and u , respectively, and subtracting, we obtain

$$\frac{d}{dr}(u u_0' - u_0 u') = k^2 u u_0. \quad (75)$$

The solutions for $V = 0$, are denoted by v and v_0 , obeying the equations

$$v'' + k^2 v = 0, \quad \text{and} \quad v_0'' = 0. \quad (76)$$

As in 75,

$$\frac{d}{dr}(v v_0' - v_0 v') = k^2 v_0 v \quad (77)$$

Subtracting 75 from 76 and integrating from $r = 0$ to ∞ we get

$$(u u_0' - u_0 u' - v v_0' + v_0 v') \Big|_{r=0}^{r=\infty} = k^2 \int_0^{\infty} (u u_0 - v v_0) dr. \quad (78)$$

Since $(u, u_0) \rightarrow (v, v_0)$ at $r \rightarrow \infty$,

$$(v v_0' - v_0 v') \Big|_{r=0} = k^2 \int_0^{\infty} (u u_0 - v v_0) dr. \quad (79)$$

We can choose the asymptotic form of v as

$$v = C \sin(kr + \delta). \quad (80)$$

We also choose the normalization so that $v = 1$ at $r = 0$. Thus $C = 1/\sin \delta$ and

$$u(r) \xrightarrow{r \rightarrow \infty} v(r) \equiv \frac{\sin(kr + \delta)}{\sin \delta}. \quad (81)$$

The solution for v_0 is a straight-line and

$$u_0(r) \xrightarrow{r \rightarrow \infty} v_0(r) \equiv D(r - a).$$

With $v_0(0) = 1$,

$$v_0(r) \equiv 1 - \frac{r}{a}. \quad (82)$$

Now, Eq. 79 becomes

$$-\frac{1}{a} - k \cot \delta = k^2 \int_0^\infty (uu_0 - vv_0) dr \quad (83)$$

For $r > a$, $u \rightarrow v$ and $v \rightarrow v_0$ slowly. For $r < a$ $u \approx u_0$, $v \approx v_0$ if E is small. Then we define the effective range r_0 that

$$r_0 = 2 \int_0^\infty (v_0^2 - u_0^2) dr. \quad (84)$$

In terms of the effective range, Eq. 83 becomes approximately,

$$k \cot \delta = -\frac{1}{a} + r_0 \frac{k^2}{2}. \quad (85)$$

Using this in 69, we find

$$\sigma = \frac{4\pi}{k^2 + (1/a - r_0 k^2/2)^2}. \quad (86)$$

In a general scattering experiment of neutrons on protons, or vice-versa, the neutron beam has its spin randomly oriented and the n-p system is in a triplet (spin parallel) and singlet (spin antiparallel) states in proportion to the corresponding weight factors for these states, which are, respectively, 3/4 and 1/4. The total scattering cross section consists of two parts

$$\sigma_{sc} = \frac{3}{4} \sigma_t + \frac{1}{4} \sigma_s. \quad (87)$$

For σ_t and σ_s we can write solutions of the form 86. We thus have to consider four parameters, a_t , σ_{0t} , a_s and σ_{0s} to describe n-p scattering at low energies.

7 Shell model + single-particle correlations

Three-body calculations become increasingly more complicated as the details of the interaction are considered. It is thus useful to study a simpler problem based on single particle model with correlations. This has been done by Bertsch and Esbensen [6]. In a single-particle approach including correlations one solves the same Hamiltonian

as in Eq. 40, but the basis of the calculations are single-particle wavefunctions for the nucleons, obtained by solving the single-particle Hamiltonian (the recoil of the core is neglected here)

$$\left[-\frac{\hbar^2}{2m} \nabla^2 + V(r) \right] \psi_i(\mathbf{r}) = \epsilon_i \psi_i(\mathbf{r}). \quad (88)$$

The single-particle potential, including spin-orbit, is parametrized in the usual way [7]

$$V(r) = -V_0 \left(1 - 0.44 r_0^2 (\mathbf{l} \cdot \mathbf{s}) \frac{1}{r} \frac{d}{dr} \right) \left[1 + \exp \left(\frac{r - R}{a} \right) \right]^{-1} \quad (89)$$

with $a = 0.67$ fm, $R = r_0(A - 2)^{1/3}$ and $r_0 = 1.27$ fm, appropriate for ^{11}Li . Note that the radius R is calculated as a function of the core mass, $A - 2$. For the protons this potential is supplemented with the Coulomb interaction with the other $(Z - 1)$ protons, represented by a uniformly charged sphere.

The strength of the potential for core nucleons is adjusted to give a reasonable estimate of the binding of the $1p_{3/2}$ proton and neutron states in p -shell nuclei which contain $N = 8$ neutrons. This leads to

$$V_0 = \left(52 - 33 \frac{N - Z}{A} \tau_3 \right) \text{ MeV} \quad (90)$$

where $\tau_3 = 1/2$ ($-1/2$) for neutrons (protons). This is very close to the value commonly used [7].

For the valence neutrons the strength of the single-particle potential is adjusted so that the resonant $p_{1/2}$ state appears at the energy $E_r = 800$ keV, which is achieved for $V_0 = 30.2$ MeV.

The effective interaction (medium modified) between the valence neutrons is taken as a density dependent delta interaction.

$$v_{\text{eff}}(\mathbf{r}_1, \mathbf{r}_2) = \delta(\mathbf{r}_1, \mathbf{r}_2) \left\{ v_0 + v_\rho \left[\rho_c \left(\frac{\mathbf{r}_1 + \mathbf{r}_2}{2} \right) / \rho_0 \right]^P \right\}. \quad (91)$$

The delta interaction form simplifies the calculation greatly. v_0 is chosen to simulate the interaction between free nucleons. The density dependent term contains the ratio of the core density, $\rho_c(r)$, and the nuclear matter density, $\rho_0 = 0.16 \text{ fm}^{-3}$. v_ρ and P are adjusted so that the pairing energies in p -shell nuclei are reasonably well reproduced.

A zero-range interaction lead to divergencies. I.e., an infinite number of momenta are present in the Fourier transform of $\delta(\mathbf{r})$. A zero-range interaction is only meaningful as effective interaction within a truncated space of states.

To understand how to handle with a truncated space let us neglect the density dependent term in 91 for the moment. The Schrödinger equation for relative motion of the valence neutrons, with reduced mass $m/2$, is

$$\left(-\frac{\hbar^2}{m} \nabla^2 + v_0 \delta(\mathbf{r}) \right) \psi(\mathbf{r}) = E \psi(\mathbf{r}). \quad (92)$$

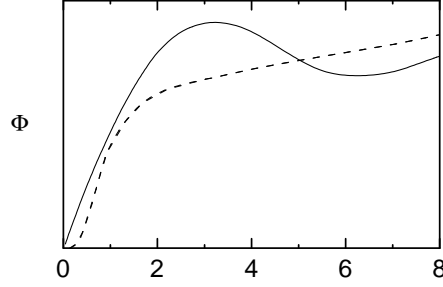


Figure 3 Radial wavefunction for the relative motion of two neutrons. The fully drawn curve is the sine-integral function $Si(k, r)$, obtained from the local pairing interaction eq. 97, which reproduces a bound state at zero energy. The dashed curve is the result obtained from the Reid soft-core potential.

The formal solution is

$$\psi(\mathbf{r}) = \psi^{(0)}(\mathbf{r}) - \int d^3r' G_0(\mathbf{r}, \mathbf{r}', E) v_0 \delta(\mathbf{r}') \psi(\mathbf{r}') \quad (93)$$

G_0 is the Green's function in the truncated space, i.e., $\epsilon_k \leq E_c$ or $k \leq k_c$,

$$G_0(\mathbf{r}, \mathbf{r}', E) = \frac{1}{(2\pi)^3} \int_{\epsilon_k \leq E_c} d^3k \frac{e^{i\mathbf{k} \cdot (\mathbf{r} - \mathbf{r}')}}{\epsilon_k - E}. \quad (94)$$

To simulate the fact that the scattering length for free neutrons is very large we require that 93 has a bound state solution at zero energy. This implies that $\psi^{(0)} = 0$ ($\psi^{(0)}$ = the solution of the equation without the interaction). At $\mathbf{r} = 0$

$$1 = -\frac{v_0}{(2\pi)^3} \int_{\epsilon_k \leq E_c} d^3k \frac{1}{\epsilon_k} \quad (95)$$

which implies that

$$v_0 = -2\pi^2 \left(\frac{\hbar^2}{m} \right)^{3/2} E_c^{-1/2}. \quad (96)$$

Choosing $E_c = 40$ MeV (\sim Fermi energy of a usual nucleus) one gets $v_0 = -831$ MeV fm³. Using 93, 95 and 96 the bound state wavefunction at zero energy is

$$\psi_{E=0}(\mathbf{r}) = \psi(0) \frac{Si(k_c r)}{k_c r} \quad (97)$$

where $Si(x) = \int_0^x dt \sin(t)/t$. This wave function, $Si(k_c r)$, (solid line) is shown in Fig. 3, together with the radial wavefunction obtained from a commonly used finite range interaction, namely the Reid soft core potential [8] (dashed curve). The agreement is quite reasonable.

The wavefunctions of the core nucleons are needed only to construct the core-density, to be used in 93. They are constructed by using the single-particle wavefunction obtained from 88 and 89,

$$\psi_{n\ell jm}(\mathbf{r}) = \phi_{n\ell j}(r) \sum_{m_\ell, m_s} (\ell m_\ell 1/2 m_s | jm) Y_{\ell m}(\hat{\mathbf{r}}) \chi_{m_s}. \quad (98)$$

The neutron-neutron wave function is obtained by coupling these solutions to the total angular momentum J . What is needed are the two-particle wavefunction at $\mathbf{r}_1 = \mathbf{r}_2 \equiv \mathbf{r}$ to compute the effect of the zero-range residual interaction, Eq. 91.

For example, coupling to $J = 0$ yields the two-particle wavefunction

$$\begin{aligned} \psi_{nn'\ell j}^{(2)}(\mathbf{r}) &= \frac{\phi_{n\ell j}(r)\phi_{n'\ell j}(r)}{\sqrt{4\pi}} (-1)^\ell \sqrt{\frac{2\ell+1}{8\pi}} \\ &\times \frac{1}{\sqrt{2}} \left(\chi_{1/2}^{(1)}\chi_{-1/2}^{(2)} - \chi_{-1/2}^{(1)}\chi_{1/2}^{(2)} \right). \end{aligned} \quad (99)$$

The spin part is seen to be an $S = 0$ state, which is typical when $\mathbf{r}_1 = \mathbf{r}_2 \equiv \mathbf{r}$, since the spatial part is automatically symmetric and the whole wavefunction has to be antisymmetric. The wavefunction for $J \neq 0$ is a bit more complicated [6].

The single-particle wavefunctions $\phi_{n\ell j}(r)$ are bound states as well as continuum states, but bound states occupied by the core nucleons are explicitly excluded from the space. This procedure is equivalent to solve the Bethe-Goldstone equation [7] for the two valence neutrons in the presence of the core.

One can find the eigenfunctions and energies of the two-particle Hamiltonian, Eq. 20, by expanding in terms of the basis $\psi_J^{(2)}$ followed by diagonalization. However, a more numerically interesting approach reported in Ref. [6].

The two-particle Green's function is defined as

$$G_2^{(0)}(E) = \frac{1}{H_2^{(0)} - E - i\eta} = \sum_{2p} \frac{|2p\rangle\langle 2p|}{\epsilon_{2p}^{(0)} - E - i\eta} \quad (100)$$

in the space of two-particle states $|2p\rangle$ with energies $\epsilon_{2p}^{(0)}$.

The correlated two-particle Green's function is (with the residual interaction)

$$G_2(E) = (H_2 - E - i\eta)^{-1} = \sum_{\widetilde{2p}} \frac{|\widetilde{2p}\rangle\langle \widetilde{2p}|}{\epsilon_{\widetilde{2p}} - E - i\eta} \quad (101)$$

where $|\widetilde{2p}\rangle$ are the correlated two-particle states, with eigenvalues $\epsilon_{\widetilde{2p}}$. H_2 is Eq. 20.

We note that

$$1 + G_2^{(0)}(E)v_{\text{eff}} = G_2^{(0)}(H_2^{(0)} + v_{\text{eff}} - E - i\eta) = G_2^{(0)}(E)G_2^{-1}(E) \quad (102)$$

or

$$G_2(E) = \left(1 + G_2^{(0)}(E)v_{\text{eff}}\right)^{-1} G_2^{(0)}(E). \quad (103)$$

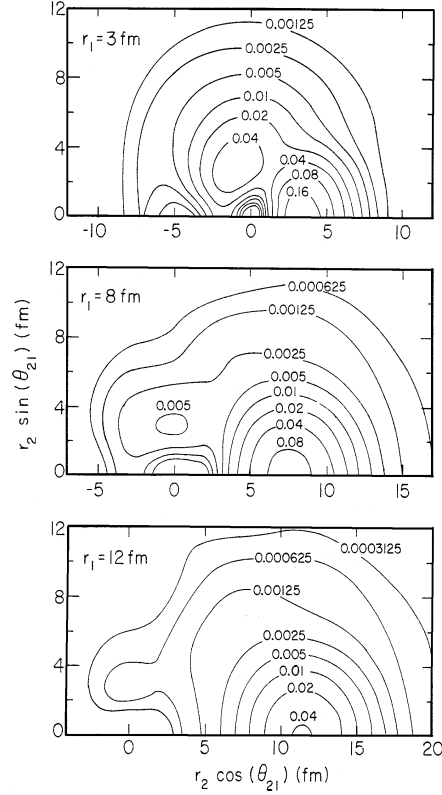


Figure 4 Contour plots of the two-particle density of the valence neutrons in ^{11}Li . The density has been weighted by $4\pi r_1^2 4\pi r_2^2$, and it is illustrated (in units of fm^{-2}) for three different positions r_1 of one of the neutrons. The contours are shown as functions of the coordinates $r_2 \cos(\theta_{12})$, $r_2 \sin(\theta_{12})$ of the second netutron.

Thus

$$\langle 2p_0 | \delta(\mathbf{r}_1 - \mathbf{r}_2) G_2(E) | 2p \rangle = \sum_{\widetilde{2p}} \frac{\langle 2p_0 | \delta(\mathbf{r} - \mathbf{r}_2) | \widetilde{2p} \rangle \langle \widetilde{2p} | 2p \rangle}{\epsilon_{2p} - E - i\eta} \quad (104)$$

$$= \frac{\langle 2p_0 | \delta(\mathbf{r}_1 - \mathbf{r}_2) (1 + G_2^{(0)}(E) v_{\text{eff}})^{-1} | 2p \rangle}{\epsilon_{2p}^{(0)} - E - i\eta} \quad (105)$$

where we used Eqs. 100, 101, and 103.

Eqs. 104 and 105 solve the problem. 104 diverges when E is identical to one of the correlated energy eigenvalues. Keeping a finite (but small) η , the imaginary part of this expression will have a local maximum when E coincides with an eigenvalue. A simple numerical search can be made to locate the ground state energy of the pair.

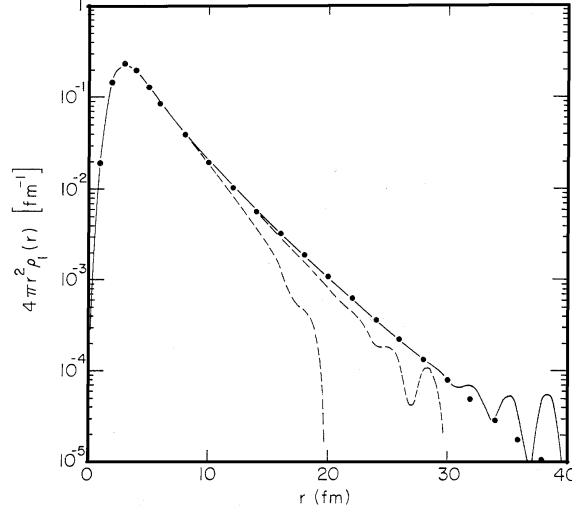


Figure 5 Single particle density of the valence neutrons in ^{11}Li , weighted by $4\pi r^2$. The radial cutoff is 20 and 30 fm for the two dashed curves, and it is 40 fm for the fully drawn curve. The dots represent the best $p_{3/2}$ shell model fit.

The amplitudes of the ground-state wavefunction on two-particle shell model states can also be extracted. Eqs. 104 and 105 show that

$$\langle 2\tilde{p}|2p\rangle = N \text{Im} \frac{\langle 2p_0|\delta(\mathbf{r}_1 - \mathbf{r}_2) [1 + G_2^{(0)}(E)v_{\text{eff}}]^{-1} |2p\rangle}{\epsilon_{2p}^{(0)} - E - i\eta} \quad (106)$$

when E is set equal to the ground state energy of the pair. N is a constant that can be eliminated by the normalization of the ground state wavefunction. The state $|2p_0\rangle$ is fixed in this process but it can otherwise be any of the two-particle states.

The local independent two-particle Green's function can be constructed from the two-particle states, e.g., Eq. 99. For a pair coupled to $J = 0$ one gets [6]

$$G_2^{(0)}(\mathbf{r}, \mathbf{r}'E) = \sum_{nn'l_j} \frac{\phi_{nl_j}(r)\phi_{n'l_j}(r)\phi_{nl_j}(r')\phi_{n'l_j}(r')}{\epsilon_{nl_j} + \epsilon_{n'l_j} - E - i\eta} \times \frac{2j+1}{8\pi} Y_{00}(\hat{\mathbf{r}})Y_{00}(\hat{\mathbf{r}}'). \quad (107)$$

The main complication to calculate 107 is the inversion of the operator $1 + G_2^{(0)}(E)v_{\text{eff}}$. This inversion is similar to the one used in ordinary RPA theory [9], and it can be performed on a finite radial grid.

The numerical results depend on the choice of the parameters v_ρ and P in Eq. 91. These parameters were chosen to fit the two-neutron binding energies of ^{11}C

and ^{12}Be , which like ^{11}Li have eight valence neutrons. The best fit [6] is obtained for $P = 1.2$ and $v_p = 930 \text{ MeV fm}^3$.

The two-particle wavefunctions $|\widetilde{2p}\rangle \equiv \psi^{(2)}(\mathbf{r}_1, \mathbf{r}_2)$ are obtained by solving Eqs. 104 and 105 for the eigenvalues and correlated amplitudes, respectively. That is, using Eq. 99 the non-correlated two particle wavefunctions $|2p\rangle \equiv \psi_{nn'j}^{(2)}(\mathbf{r}, \mathbf{r})$ are constructed (see Appendix A of [6]). Then the correlated two-particle wavefunction

$$\psi_{g.s}(\mathbf{r}_1, \mathbf{r}_2) = \sum_{nn'\ell_j} \alpha_{nn'\ell_j} \Psi_{nn'j}^{(2)}(\mathbf{r}_1, \mathbf{r}_2) \quad (108)$$

is constructed. The $\alpha_{nn'\ell_j}$ are then found by the Green's function method, as described above.

In Figure 4 we see the two-particle density $\rho^{(2)}(r_1, r_2, \theta_{21})$ obtained from the correlated two-particle wavefunction. r_1 and r_2 are the radial coordinates of the neutrons with respect to the core and θ_{21} is the angle between them. The density has been weighted by $4\pi r_1^2 4\pi r_2^2$.

When one of the particles is required to be close to the core (upper part of Fig. 4) there are two peaks in $\rho^{(2)}$, one is close to the selected particle and one is at $\theta_{21} = 90^\circ$. The later peak is associated with the $S = 1$ component of the two-particle wavefunction whereas the peak near the particle is dominated by the $S = 0$ component. When one of the particles is far away from the core (lower part of the Figure) the peak at $\theta_{21} = 90^\circ$ almost disappears.

The single particle density is obtained from $\rho^{(2)}$ by integration over one of the variables, e.g., \mathbf{r}_2 . In figure 5 the single particle density $\rho^{(1)}(r)$ weighted by $4\pi r^2$ is plotted against r . The long dashed, short-dashed, and the solid curve are obtained by increasing the radial cutoff of the numerical integration for 20, 30 and 40 fm, respectively. The dots are obtained from the density of a $p_{1/2}$ bound state in a Woods-Saxon potential of form 89, with $r_0 = 1.52$ fm and $V_0 = 26.53$ MeV. This yields a single-particle energy of -0.296 MeV, not far from the two-particle binding energy.

One can compare the results obtained via the Green's function method [6] with the variational three-body calculations presented in the last Section [5]. The variables ρ and λ are here equivalent to $\mathbf{r}_1 - \mathbf{r}_2$ and $\frac{1}{2}(\mathbf{r}_1 + \mathbf{r}_2)$ (see Fig. 6(b)). One finds

$$\langle r^2 \rangle = 39 \text{ fm}^2, \quad \langle \rho^2 \rangle = 43 - 54 \text{ fm}^2 \quad (109)$$

$$\frac{1}{4} \langle |\mathbf{r}_1 + \mathbf{r}_2|^2 \rangle = 24.4 \text{ fm}^2, \quad \langle \psi^2 \rangle = 21 - 28 \text{ fm}^2 \quad (110)$$

where the range of $\langle \rho^2 \rangle$ and λ^2 from Ref. [5] depend on their choices for the potential parameters. The agreement is quite reasonable. Based on the results of Bertsch and Esbensen [6] one concludes that the di-neutron model for ^{11}Li has at least qualitative validity.

The Green's function method [6] is a very handy, technically simple, method to quickly assess the characteristics of a three-body system. However, the model ignores finite-range (and hence p -wave) effects in pairing interactions. The simplicity of the

model is lost if a delta interaction between the valence neutrons is not used. The recoil of the core is also not treated properly. Thus, while reasonable for ${}^9\text{Li}+n+n$ (${}^{11}\text{Li}$) it is a bad approximation for ${}^4\text{He}+n+n$ (${}^6\text{He}$).

Supplement D

8 Scattering states and resonances

The total cross section for a scattering process is given by

$$\sigma_t = \sigma_{sc} + \sigma_r \quad (111)$$

where σ_{sc} is the elastic scattering cross section treated in the Supplement C. To derive an expression for the reaction cross section we use

$$\begin{aligned} e^{ikz} &= \sum_{\ell=0}^{\infty} i^{\ell} (2\ell+1) j_{\ell}(kr) P_{\ell}(\cos \theta) \\ &\sim \sum_{\ell} \frac{i^{\ell+1}}{2kr} (2\ell+1) \left\{ \exp \left[-i \left(kr - \frac{\ell\pi}{2} \right) \right] \right. \\ &\quad \left. - \exp \left[i \left(kr - \frac{\ell\pi}{2} \right) \right] \right\} P_{\ell}(\cos \theta) \end{aligned} \quad (112)$$

for $r \rightarrow \infty$. In a reaction the scattering amplitude of the outgoing spherical wave part of the plane wave is modified. The wavefunction $\psi(r)$ describing the outgoing wave after interaction is given by

$$\begin{aligned} \psi(r) &\sim \sum_{\ell} \frac{i^{\ell+1}}{2kr} (2\ell+1) \left\{ \exp \left[-i \left(kr - \frac{\ell\pi}{2} \right) \right] \right. \\ &\quad \left. - \eta_{\ell} \exp \left[i \left(kr - \frac{\ell\pi}{2} \right) \right] \right\} P_{\ell}(\cos \theta) \end{aligned} \quad (113)$$

for $r \rightarrow \infty$.

We can write $\eta_{\ell} = |\eta_{\ell}| e^{2i\delta_{\ell}}$. If $|\eta_{\ell}| = 1$ the scattering is elastic. If $|\eta_{\ell}| < 1$, then both elastic scattering and reaction will occur. The elastic scattered wavefunction is the difference between 112 and 113

$$\psi_{sc} = \sum_{\ell} \frac{i^{\ell+1}}{2kr} (2\ell+1) (1 - \eta_{\ell}) \exp \left[i \left(kr - \frac{\ell\pi}{2} \right) \right] P_{\ell}(\cos \theta). \quad (114)$$

Using the same steps as in 59 – 61 we find

$$\frac{d\sigma_{sc}(\theta)}{d\Omega} = \frac{\pi}{k^2} \left| \sum_{\ell=0}^{\infty} \sqrt{2\ell+1} (1 - \eta_{\ell}) Y_{\ell 0}(\theta) \right|^2$$

and

$$\sigma_{sc} = \int \frac{d\sigma_{sc}}{d\Omega} d\Omega = \sum_{\ell=0}^{\infty} \sigma_{sc,\ell} \quad (115)$$

where

$$\sigma_{sc,\ell} = \frac{\pi}{k^2} (2\ell + 1) |1 - \eta_\ell|^2. \quad (116)$$

To calculate the total reactions cross section we use Eq. 58 to obtain the flux of particles towards a sphere of radius r . The next flux will be the number of particles removed from the beam. Thus we have to use $\psi = e^{ikz} + \psi_{sc}$ in 60. It is left to the reader to show that

$$S_r = \frac{\hbar\pi}{\mu k} \sum_{\ell} (2\ell + 1) (1 - |\eta_\ell|^2).$$

Therefore, the total reaction cross section is

$$\sigma_r = \frac{S_r}{v} = \sum_{\ell=0}^{\infty} \sigma_{r,\ell} \quad (117)$$

where

$$\sigma_{r,\ell} = \frac{\pi}{k^2} (2\ell + 1) \{1 - |\eta_\ell|^2\}. \quad (118)$$

The total cross section is

$$\begin{aligned} \sigma = \sigma_{sc} + \sigma_r &= \frac{\pi}{k^2} (2\ell + 1) \{|1 - \eta_\ell|^2 + 1 - |\eta_\ell|^2\} \\ &= \frac{2\pi}{k^2} (2\ell + 1) \{1 - \text{Re} \eta_\ell\}. \end{aligned} \quad (119)$$

When there is no reaction, $|\eta_\ell|^2 = 1$. Since $\eta_\ell = |\eta_\ell|e^{2i\delta_\ell}$, this means purely real δ_ℓ . In the case of any reaction, at least one of the δ_ℓ is complex, so $|\eta_\ell| < 1$. This is because the outgoing particles cannot exceed the number of incident particles.

Therefore, the maximum value of $\sigma_{sc,\ell}$ is obtained for

$$\eta_\ell = -1 : \quad \sigma_{sc,\ell,\text{max}} = \frac{4\pi}{k^2} (2\ell + 1) \quad (120)$$

and $\sigma_{r,\ell} = 0$.

The maximum value of $\sigma_{r,\ell}$ is for $\eta_\ell = 0$, in which case $\sigma_{sc,\ell} \neq 0$. This means that there is *no reaction without scattering*.

For scattering on an object with a sharp edge with radius R we can say that all particles with

$$\ell < \frac{pR}{\hbar} = kR \quad (121)$$

will react with the target. Thus, $\eta_\ell \cong 0$ for $\ell < kR$ and $\eta_\ell = 1$ for $\ell > kR$. We obtain

$$\sigma_r \cong \frac{\pi}{k^2} \sum_{\ell=0}^{kR} (2\ell + 1) = \pi(R + 1/k)^2 \cong \pi R^2$$

for $kR \gg 1$ (wavelength much smaller than the radius). Similarly, for the scattering cross section

$$\sigma_{sc} \cong \pi R^2. \quad (122)$$

The total cross section is

$$\sigma_T \cong 2\pi R^2. \quad (123)$$

And is twice the classical cross section, πR^2 . This is due to the extra-piece arising from the scattering cross section 122. The wave is diffracted around the target and this takes out flux from the incident wave, resulting in 122. This extreme limit, valid for $kR \gg 1$ (high energies) is called by shadow scattering.

8.1 Breit-Wigner formula for $\ell = 0$

In Supplement C we found that

$$\lim_{k \rightarrow 0} \frac{\delta}{k} = -a_k \quad (124)$$

$$k \cot \delta = -\frac{1}{a_k} + \frac{r_0 k^2}{2}. \quad (125)$$

We now define

$$k \cot \delta = -\frac{1}{a(k)} \quad (126)$$

for all values of k . If there is no reaction, $a(k)$ is real. For $\sigma_r \neq 0$ $a(k)$ is in general complex.

Denoting now $a(k) = a$,

$$\begin{aligned} \eta &= e^{i2\delta} = (\cos \delta + i \sin \delta)^2 \\ &= \left(\frac{1 - ika}{\sqrt{1 + k^2 a^2}} \right) = \frac{1 - ika}{1 + ika}. \end{aligned} \quad (127)$$

Thus, for $\ell = 0$,

$$\sigma_{sc} = \frac{\pi}{k^2} |1 - \eta| = \frac{4\pi}{|1/a + ik|^2} \quad (128)$$

$$\sigma_r = \frac{\pi}{k^2} (1 - |\eta|^2) = \frac{\text{Im}(1/a)}{|1/a + ik|^2}. \quad (129)$$

For real a , σ_r is zero. In this situation, and resonance energy E_0 , the phase shift $\delta \sim \pi/2$, so that

$$\frac{1}{a(E_0)} = 0. \quad (130)$$

Expanding $1/a(E)$ about E_0 , we get

$$\frac{1}{a(E)} = 0 + (E - E_0) \left[\frac{d}{dE} \left(\frac{1}{a} \right) \right]_{E_0} + \dots \quad (131)$$

Defining,

$$\left[\frac{d}{dE} \left(\frac{1}{a} \right) \right]_{E_0} = \frac{2k}{\Gamma_s} \quad (132)$$

we find

$$\sigma_{sc} = \frac{4\pi}{|(E - E_0)^2 2k/\Gamma_s + ik|^2} = \frac{(\pi/k^2)\Gamma_s^2}{|(E - E_0) + i\Gamma_s/2|^2} = \frac{(\pi/k^2)\Gamma_s^2}{(E - E_0)^2 + \Gamma_s^2/4}. \quad (133)$$

This is known as a *Breit-Wigner formula*.

To derive an expression for the reaction cross section we keep in mind that $a(E)$ is a complex function and assuming that $1/a(E'_0) = 0$ for $E'_0 = E_0 - i\Gamma_R/2$, and defining

$$\operatorname{Re} \left[\frac{d}{dE} \left(\frac{1}{a} \right) \right]_{E'_0} = \frac{2k}{\Gamma_S} \quad ; \quad \operatorname{Im} \left[\frac{d}{dE} \left(\frac{1}{a} \right) \right]_{E'_0} = k\alpha$$

we find that

$$\begin{aligned} \frac{1}{a(E)} &= \left(E - E_0 + \frac{i\Gamma_R}{2} \right) \left(\frac{2k}{\Gamma_S} + ik\alpha \right) \\ &= \frac{2k}{\Gamma_S} (E - E_R) + ik \left[\frac{\Gamma_R}{\Gamma_S} + \alpha(E - E_0) \right] \end{aligned} \quad (134)$$

where

$$E_R = E_0 + \frac{\alpha\Gamma_R\Gamma_S}{4}. \quad (135)$$

The scattering cross section is now

$$\sigma_{sc} = \frac{4\pi}{\left| \frac{1}{a} + ik \right|^2} = \frac{(\pi/k^2)\Gamma_S^2}{(E - E_R)^2 + [\Gamma_S + \Gamma_R + \alpha\Gamma_S(E - E_0)]^2/4}. \quad (136)$$

For a sharp resonance α is small, and 136 becomes

$$\sigma_{sc} = \frac{(\pi/k^2)\Gamma_R\Gamma_S}{(E - E_R)^2 + (\Gamma_S + \Gamma_R)^2/4}. \quad (137)$$

Using 134 in 129, the reaction cross section is

$$\sigma_r = \frac{(\pi/k^2) [\Gamma_R\Gamma_S + \alpha\Gamma_S^2(E - E_0)]}{(E - E_R)^2 + [\Gamma_S + \Gamma_R + \alpha\Gamma_S(E - E_0)]^2/4}. \quad (138)$$

Again neglecting $\alpha(E - E_0)$ we obtain

$$\sigma_r = \frac{(\pi/k^2)\Gamma_R\Gamma_S}{(E - E_R)^2 + (\Gamma_S + \Gamma_R)^2/4}. \quad (139)$$

To get an insight of these formulas, let us assume a scattering by a potential such that $V(r) = 0$ for $r > R$. The radial wavefunction can be written as

$$r\psi(r) = u(r) = u_{\text{out}}(r) + u_{\text{in}}(r) \quad (140)$$

where

$$u_{\text{out}}(r) = u^{(+)} \exp(ikr), \quad \text{and} \quad u_{\text{in}}(r) = u^{(-)} \exp(-ikr). \quad (141)$$

For $r \geq R$ we know that

$$\begin{aligned} \psi(r \geq R) &= \frac{\sqrt{\pi}}{kr} \sum_{\ell} i^{\ell+1} \sqrt{2\ell+1} \left\{ \exp \left[-i \left(kr - \frac{\ell\pi}{2} \right) \right] \right. \\ &\quad \left. - \eta_{\ell} \exp \left[i \left(kr - \frac{\ell\pi}{2} \right) \right] \right\} Y_{\ell 0}(\theta). \end{aligned} \quad (142)$$

The radial wavefunction for $\ell = 0$ is ($r \geq R$)

$$(r\psi)_{\ell=0} = u(r) = \frac{\sqrt{\pi}}{k} i \{ \exp(-ikr) - \eta \exp(ikr) \}. \quad (143)$$

Comparing 140 with 143, we find

$$u^{(+)} = -\frac{\sqrt{\pi}}{k} i\eta, \quad \text{and} \quad u^{(-)} = \frac{\sqrt{\pi}}{k} i. \quad (144)$$

Now

$$\eta = \frac{-u^{(+)}(\infty)}{u^{(-)}(\infty)} = \frac{-u_{\text{out}}(R)e^{-ikR}}{u_{\text{in}}(R)e^{ikR}} \equiv \eta(R)e^{-2ikR} \quad (145)$$

where

$$\eta(R) = -\frac{u_{\text{out}}(R)}{u_{\text{in}}(R)}. \quad (146)$$

From 127, $\eta = (1 - ika) / (1 + ika)$. If we now define $a(R)$ so that

$$\eta(R) = \frac{1 - ika(R)}{1 + ika(R)} \quad (147)$$

we get

$$a(R) = \frac{1}{ik} \frac{1 - \eta(R)}{1 + \eta(R)}. \quad (148)$$

We note that

$$\left[\frac{ru'(r)}{u(r)} \right]_{r=R} = R \frac{-ik e^{-ikR} - ik\eta e^{ikR}}{e^{-ikR} - \eta e^{ikR}} = -\frac{R}{a(R)}. \quad (149)$$

As in 129 we get, using 145 and 148,

$$\sigma_r = \frac{\pi}{k^2} (1 - |\eta|^2) = \frac{4\pi}{k} \frac{\text{Im} \left(\frac{1}{a(R)} \right)}{\left| \frac{1}{a(R)} + ik \right|^2}. \quad (150)$$

Thus, the reaction cross section is a function of $a(R)$ which depends on the wavefunction at $r = R$ through Eq. 149. Well below the resonance and far from the zero of $1/a(R)$, we find $\sigma_r \sim 1/k \sim 1/v$. This is the well known “ $1/v$ law”.

In terms of $a(R)$ the scattering cross section is

$$\begin{aligned}
\sigma_{sc} &= \frac{\pi}{k^2} |1 - \eta|^2 = 4\pi \left| \frac{1 - \eta}{2ik} \right|^2 \\
&= 4\pi \left| \frac{e^{2ikR} - 1}{2ik} + \frac{1}{\frac{1}{a(R)} + ik} \right|^2 \\
&= 4\pi \left| \frac{e^{ikR} \sin kR}{k} + \frac{1}{\frac{1}{a(R)} + ik} \right|^2. \tag{151}
\end{aligned}$$

The first term is called by *potential scattering amplitude* whereas the second term is the *resonance scattering amplitude*. We recall that in terms of a , rather than $a(R)$, the scattering amplitude is given by Eq. 128.

We can again define behavior of 151 near a resonance by expanding $a(R)$ as in 131. Since

$$\left[\frac{d}{dE} \left(\frac{1}{a} \right) \right]_{E_0} = \frac{2k}{\Gamma_S} > 0 \tag{152}$$

since $\Gamma_S > 0$, we have that, below the resonance $1/a < 0$. For low energies

$$\frac{e^{ikr} \sin kR}{k} \cong R > 0.$$

Therefore, for low-energy scattering, we have destructive interference with the potential amplitude below the resonance and constructive interference above.

Away from the resonance, $a(R) \rightarrow 0$ and the second term in Eq. 151 $\simeq 0$, leaving only the first term to contribute to the scattering cross section. In this case ($a(R) \sim 0$), Eq. 149 gives $u(r = R) \cong 0$, the boundary condition for an almost impenetrable sphere. Thus for low energies, $kR \ll 1$, Eq. 151 gives $\sigma_{sc} \cong (4\pi/k^2) \sin^2 kR \cong 4\pi R^2$, the potential scattering for a rigid sphere.

Near a resonance $a(R) \rightarrow \infty$, which means that $u'(R) = 0$. This indicates that the amplitude of the incident wave is a maximum at the surface, and the continuity conditions require the same for the internal wave function.

8.2 Breit Wigner formula for all ℓ

If $V(r) \cong 0$ for $r > R$ we define

$$f_\ell = R \left(\frac{1}{u_\ell} \frac{du_\ell}{dr} \right)_{r=R} \tag{153}$$

where u_ℓ satisfies the equation

$$\frac{d^2 u_\ell}{dr^2} + \left(k^2 - \frac{\ell(\ell+1)}{r^2} \right) u_\ell(r) = 0. \tag{154}$$

The solution can be written as

$$u_\ell(r) = a_+ u_\ell^{(+)}(r) + a_- u_\ell^{(-)}(r) \quad (155)$$

with

$$\begin{aligned} u_\ell^{(\pm)}(r) &= \pm ikr [j_\ell(kr) \pm in_\ell(kr)] \\ &= ikr \begin{cases} h_\ell^{(1)}(kr) \\ -h_\ell^{(2)}(kr) \end{cases} \\ &\sim \exp \left[\pm i \left(kr - \frac{\ell\pi}{2} \right) \right] \quad \text{for } r \rightarrow \infty. \end{aligned} \quad (156)$$

[For $\ell = 0$, $u_0(r) = a_+ e^{ikr} + a_- e^{-ikr}$].

Comparing 113 with 155, using 156, we find

$$\eta_\ell = -\frac{a_+}{a_-}. \quad (157)$$

Now,

$$f_\ell = R \frac{a_+ u_\ell'^{(+)}(R) + a_- u_\ell'^{(-)}(R)}{a_+ u_\ell^{(+)}(R) + a_- u_\ell^{(-)}(R)}. \quad (158)$$

Using the definition

$$\left[R \frac{1}{u_\ell^{(\pm)}} \frac{du_\ell^{(\pm)}}{dr} \right]_{r=R} = S_\ell \pm i\mathcal{K}_\ell; \quad [S_0 = 0, \mathcal{K}_0 = kr]$$

and 157 we get

$$\eta_\ell = \frac{f_\ell - S_\ell + i\mathcal{K}_\ell}{f_\ell - S_\ell - i\mathcal{K}_\ell} = \left(1 + \frac{2i\mathcal{K}_\ell}{f_\ell - S_\ell - i\mathcal{K}_\ell} \right) e^{2i\xi_\ell} \quad (159)$$

where

$$\frac{u_\ell^{(-)}(R)}{u_\ell^{(+)}(R)} = e^{2i\xi_\ell}; \quad [\xi_0 = -kR]. \quad (160)$$

Using 116 and 119 we find

$$\sigma_{sc} = \frac{\pi}{k^2} \sum_\ell |A_\ell(\text{pot}) + A_\ell(\text{res})|^2 \quad (161)$$

where

$$A_\ell(\text{pot}) = e^{-2i\xi_\ell} - 1 \quad (162)$$

$$A_\ell(\text{res}) = \frac{-2i\mathcal{K}_\ell}{f_\ell - S_\ell - i\mathcal{K}_\ell} \quad (163)$$

Also,

$$\sigma_r = \frac{\pi}{k^2} \sum_\ell \frac{(2\ell + 1) \cdot 2\mathcal{K}_\ell (f_\ell - f_\ell^*)}{\left[\frac{1}{2} (f_\ell + f_\ell^*) - S_\ell \right]^2 + \left[\frac{1}{2} (f_\ell - f_\ell^*) - \mathcal{K}_\ell \right]^2}. \quad (164)$$

For an impenetrable sphere, $u_\ell(R) = 0$. Then from Eq. 158, $f_\ell \rightarrow \infty$ and therefore $A_\ell(\text{res}) \rightarrow 0$. In this case $\sigma_r \rightarrow 0$.

To be more explicit let us assume that $V(r) = -V_0$ for $r < R$, then

$$u_{\text{in}}(r) = A_{\text{in}} \sin \left[Pr - \frac{\ell\pi}{2} + \alpha(E) \right], \quad r < R \quad (165)$$

$$u_{\text{out}}(r) = A_{\text{out}} \sin \left[kr - \frac{\ell\pi}{2} + \beta(E) \right], \quad r > R \quad (166)$$

where α and β are complex functions of the energy, and

$$P = \frac{\sqrt{2m(E + V_0)}}{\hbar}, \quad k = \frac{\sqrt{2mE}}{\hbar}. \quad (167)$$

From 158 and 165 we find

$$\begin{aligned} f_\ell &= PR \cot \left[PR - \frac{\ell\pi}{2} + \alpha(E) \right] \\ &= kR \cot \left[kR - \frac{\ell\pi}{2} + \beta(E) \right]. \end{aligned} \quad (168)$$

From

$$\begin{aligned} u_{\text{in}}(R) = u_{\text{out}}(R), \quad \frac{A_{\text{in}}}{A_{\text{out}}} &= \frac{\sin [kR - \ell\pi/2 + \beta(E)]}{\sin [PR - \ell\pi/2 + \alpha(E)]} \\ &= \frac{kR}{\sqrt{f_\ell^2 + k^2 R^2}} \frac{\sqrt{f_\ell^2 + P^2 R^2}}{PR} \end{aligned} \quad (169)$$

Treating f_ℓ as real, $f_\ell \gtrsim PR \rightarrow A_{\text{in}}/A_{\text{out}} \sim k/P \ll 1$, if $E \ll V_0$. But for $f_\ell = 0$, $A_{\text{in}}/A_{\text{out}} = 1$, and the particle penetrates the region of $r < R$ with the maximum amount. Thus $f_\ell = 0$ corresponds to a resonance.

We define a resonance energy formally as in

$$\text{Re} \left[f_\ell(E_r^\ell) \right] = 0. \quad (170)$$

Thus

$$f_\ell(E) = i \text{Im} f_\ell(E_r^\ell) + (E - E_r^\ell) \left(\frac{\partial f_\ell}{\partial E} \right)_{E=E_r^\ell} + \dots \quad (171)$$

and Eq. 162 yields

$$A_\ell(\text{res}) = \frac{i\Gamma_\alpha}{E - E_{\text{res}}^\ell + i\Gamma/2} \quad (172)$$

where

$$\Gamma_\alpha = \frac{-2\mathcal{K}_\ell}{(\partial f_\ell / \partial E)_{E=E_r^\ell}} \quad ; \quad \Gamma_r = \frac{2\text{Im} f_\ell(E_r^\ell)}{(\partial f_\ell / \partial E)_{E=E_r^\ell}} \quad (173)$$

$$\Gamma = \Gamma_\alpha + \Gamma_r \quad (174)$$

(175)

$$E_{\text{res}}^\ell = E_r^\ell + \frac{S_\ell}{(\partial f_\ell / \partial E)_{E=E_r^\ell}} \quad (176)$$

Γ is the total width and Γ_r is the reaction width. E_{res}^ℓ is the actual resonance energy which differs from E_r by a small amount $S_\ell / (\partial f_\ell / \partial E)_{E=E_r^\ell}$ (equal to zero for $\ell = 0$).

The expression for $\sigma_{sc}^{(\ell)}$ and $\sigma_r^{(\ell)}$ are now given by

$$\sigma_{sc}^{(0)} = \frac{\pi}{k^2} \left| \left[e^{-2ikR} - 1 \right] + \frac{i\Gamma_\alpha}{E - E_{\text{res}}^0 + i\Gamma/2} \right|^2 \quad \text{for } \ell = 0 \quad (177)$$

$$\sigma_{sc}^{(\ell)} = \frac{\pi}{k^2} (2\ell + 1) \frac{\Gamma_\alpha^2}{(E - E_{\text{res}}^\ell)^2 + (\Gamma/2)^2} \quad \text{for } \ell \geq 1 \quad (178)$$

$$\sigma_r^{(\ell)} = \frac{\pi}{k^2} (2\ell + 1) \frac{\Gamma_\alpha \Gamma_r}{(E - E_{\text{res}}^\ell)^2 + (\Gamma/2)^2}. \quad (179)$$

where in $\sigma_{sc}^{(\ell)}$ the potential scattering term is dropped and in $\sigma_{sc}^{(0)}$ we used $\xi_0 = -kR$.

Γ_r maybe interpreted as the sum of all widths except the incident channel width Γ_α

$$\Gamma_r = \sum_{\beta \neq \alpha} \Gamma_\beta, \quad \Gamma = \sum \Gamma_\beta = \Gamma_\alpha + \Gamma_r \quad (180)$$

The scattering cross section $\sigma_{\beta \leftarrow \alpha}^{(\ell)}$ from channel α into channel β is given by 173

$$\sigma_{\beta \leftarrow \alpha}^{(\ell)} = \frac{\pi}{k^2} (2\ell + 1) \frac{\Gamma_\alpha \Gamma_\beta}{(E - E_{\text{res}}^\ell)^2 + (\Gamma/2)^2}. \quad (181)$$

9 The Efimov states

^{11}Li is an example of a general class of three-body systems with a common characteristic: the three subsystem (i.e., $1 + 2$, $1 + 3$ and $2 + 3$) are “resonant”. By resonant we mean that they have resonant, almost bound states. As we have seen in Supplement A the n-n system has a resonant state (the singlet state of the deuteron) close to threshold.[†] The ^{10}Li ($^9\text{Li} - n$) system has also a resonant state at about 500 keV.

Efimov [11, 12] has shown that resonant two-body forces give rise to a series of levels in three-particle systems. For resonant systems, the range of the force r_0 is considerably smaller than the scattering length, a (see Supplement B). A barely bound (unbound) state has a very large scattering length.

For simplicity consider three spinless neutral particles of equal mass, interacting through a potential $gV(r)$, with $V(r) > 0$. At $g = g_0$ two particles get bound

[†]Due to the charge-independence of the nuclear interaction, the n-n system and the n-p system are considered to be identical.

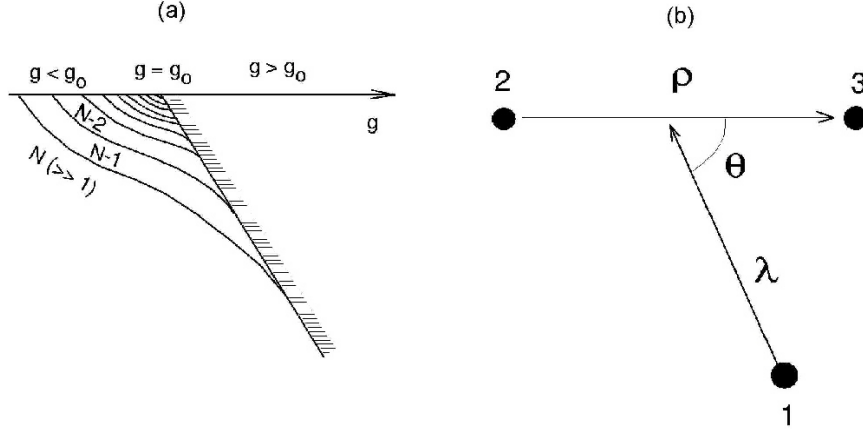


Figure 6 (a) Behavior of states of a three-body system as a function of the strength of the interaction. (b) Jacobi coordinates.

in their first s -state. For values of g close to g_0 , the two-particle scattering length a is large, and this is the region of interest. In the Figure 6 the series of levels for the three-body particle is shown. The hatched boundary is the continuum boundary .

As g grows, approaching g_0 , three-particle bound states emerge one after the other. At $g = g_0$ (infinite scattering length) their number is infinite. As g grows beyond g_0 , levels leave into the continuum one after the other.

The number of levels is given by the equation [11]

$$N \cong \frac{1}{\pi} \ln(|a|/r_0). \quad (182)$$

The physical cause for this effect is in the emergence of effective attractive long-range forces of radius a in three-body systems. One can show that they are of the $1/R^2$ kind; $R^2 = r_{12}^2 + r_{23}^2 + r_{31}^2$. With $a \rightarrow \infty$ the number of levels becomes infinite as in the case of two particles interacting with attractive $1/r^2$ potential.

These are the basic results obtained by Efimov. They are of general validity and ^{11}Li is a good example. If the di-neutron model is considered, $r_{nn} \ll r_{n-^9\text{Li}}$ and the $1/R^2$ attraction term deduced by Efimov means that the $^9\text{Li} + 2n$ -system behaves as an atom, possessing ‘‘Rydberg’’ states, with a di-neutron-core potential of the form $1/R_{2n-^9\text{Li}}^2$. As far as we know, only one of these states is known: the ground state. But other states are not ruled out. In fact, it has been shown [13] that depending on the pairing energy of the two valence neutrons, several Rydberg states may exist in ^{11}Li .

Supplement E

10 The Fadeev equations

The He atom, the ${}^3\text{H}$ and ${}^3\text{He}$ nuclei are examples of systems for which a three-body solution of the Schrödinger equation is necessary. Numerical solution is now done in a very precise manner [28]. Not only the bound states, but also scattering observable and responses to external probes are now being investigated.

There are many techniques to solve the three-body problem variational calculations [4, 30], the use of hyperspherical harmonics [29] and Green's function Monte Carlo [33]. The most commonly used method is solving the Fadeev equations [31, 32].

Let us consider three particles interacting via two-body interactions $V(r_{ij})$. The Hamiltonian is

$$H = \sum_{i=1}^3 t_i + \sum_{i<j} V(r_{ij}). \quad (183)$$

The bound state Schrödinger equation is

$$(H - E)\psi = 0. \quad (184)$$

Solving this equation amounts to obtaining the wave functions and discrete energies E_α of the bound states

It is convenient to employ the *Jacobi coordinates*

$$\boldsymbol{\rho}_i = \mathbf{r}_j - \mathbf{r}_k, \quad \text{and} \quad \boldsymbol{\lambda}_i = \frac{1}{2}(\mathbf{r}_j + \mathbf{r}_k) - \mathbf{r}_i \quad (185)$$

where r_i are the position of the three nucleons, and $i, j, k = 1, 2, 3$ are taken cyclically.

It is also convenient to use the notation

$$V_i \equiv V(\boldsymbol{\rho}_i). \quad (186)$$

The Fadeev equations are obtained by writing the Schrödinger wave function ψ as

$$\begin{aligned} \psi &= \psi_1(\boldsymbol{\rho}_1, \boldsymbol{\lambda}_1) + \psi_2(\boldsymbol{\rho}_2, \boldsymbol{\lambda}_2) + \psi_3(\boldsymbol{\rho}_3, \boldsymbol{\lambda}_3) \\ &= \psi_1 + \psi_2 + \psi_3. \end{aligned} \quad (187)$$

Substitution in 184 yields (Fadeev equations)

$$(T + V_i - E)\psi_i = -V_i(\psi_j + \psi_k); \quad i, j, k = 1, 2, 3 \quad (188)$$

with i, j, k permuted cyclically and $T = \sum_i t_i$.

For identical particles, like the $3N$ -system (i.e., ${}^3\text{H}$, ${}^3\text{He}$, etc), the $\psi_i (i = 1, 2, 3)$ amplitudes all have the same functional form so that once ψ_1 is found, the other two can be constructed by a rotational transformation. I.e., counterclockwise rotations of the particle coordinates of 185 (see also Fig. 6(b)) generate the sets

$$\boldsymbol{\rho}_3 = -\frac{1}{2}\boldsymbol{\rho}_1 - \boldsymbol{\lambda}_1, \quad \text{and} \quad \boldsymbol{\lambda}_3 = \frac{3}{4}\boldsymbol{\rho}_1 - \frac{1}{2}\boldsymbol{\lambda}_1 \quad (189)$$

and

$$\boldsymbol{\rho}_2 = -\frac{1}{2}\boldsymbol{\rho}_1 - \boldsymbol{\lambda}_1, \quad \text{and} \quad \boldsymbol{\lambda}_2 = -\frac{3}{4}\boldsymbol{\rho}_1 - \frac{1}{2}\boldsymbol{\lambda}_1. \quad (190)$$

Hence, for these systems one may focus on the solution of one of the Faddeev amplitudes, say $\psi(\boldsymbol{\rho}_1, \boldsymbol{\lambda}_1) = \psi(\boldsymbol{\rho}, \boldsymbol{\lambda})$.

For an asymmetrical three-body system, the equivalent to the Jacobi coordinates can be labelled as x and y , so that

$$x_i = \sqrt{\frac{1}{m} \frac{m_j m_k}{m_j + m_k}} (\mathbf{r}_j - \mathbf{r}_k), \quad y_i = \sqrt{\frac{1}{m} \frac{(m_j + m_k) m_i}{(m_j + m_k) + m_i}} \left(\frac{m_j \mathbf{r}_j + m_k \mathbf{r}_k}{m_j + m_k} - \mathbf{r}_i \right), \quad (191)$$

where i, j, k is a cyclic permutation of 1,2,3; m_i and r_i are the masses and coordinates of the three particles.

Summing up the three Faddeev equations gives the Schrödinger equation. The solutions of the Faddeev equations satisfy therefore also the Schrödinger equation. The opposite statement does not hold, however, since Ψ can vanish identically even when the three components Ψ_i individually are non-zero functions. Concerning the total function, Ψ , the Schrödinger and the Faddeev equations provide identical solutions.

11 Strict three-body calculations

In the last two Sections we have presented the simplest and most transparent calculations for a three-body system, e.g., ^{11}Li or ^6He . However, as we have seen, the models rely on strong assumptions. In the first the spin variables of the neutrons were neglected. In the second a delta interaction was used. These assumptions are needed for the sake of simplicity. Pauli blocking was also not included properly in the variational calculations discussed previously.

The Efimov effect was discovered theoretically as a peculiar behavior of a three-body system with short-range two-body potentials [11]. The effect appears when at least two of the binary subsystems have extremely large scattering lengths or bound states at nearly zero energy. Then a number of three-body bound states arises with enormous spatial extension and exceedingly small binding energies. Even when none of the binary subsystems is bound, the three-body system may have a large number of bound states. One surprising consequence is that *more* three-body bound states can appear by *weakening* the potentials such that the scattering lengths increase.

These states have not been seen experimentally yet, but their possible existence have been investigated theoretically in a few systems like the three ^4He -atoms (^4He -trimer) [14]. Such investigations have been rather demanding in terms of computer capacity as the extremely small binding energies and the large spatial extensions of the systems put strict requirements on the numerical accuracies. However, an efficient method was suggested for solving the Faddeev equations in coordinate space [15]. The method is particularly suitable for studying the Efimov effect.

The characteristic properties of halo nuclei off hand match the description of Efimov states rather well. The fact that they often are describable as highly

clusterized two- or three-body systems furthermore improves the resemblance.

In this Section we first describe the hyperangular function method for the Fadeev equations in some detail and discuss the asymptotic properties of the equations. Using this method we then investigate the conditions for possible existence of the Efimov effect in the two-neutron halo nuclei. We summarize the results obtained by M. Zhukov, D. Fedorov, J. Vaagen, and collaborators [1].

11.1 Hyperangular functions

The ordinary set of Jacobi coordinates $\{\mathbf{x}, \mathbf{y}\}$ does not facilitate the analysis of the asymptotic behavior of a three-body system since the boundary conditions in this set may change significantly within the two-dimensional $\{x, y\}$ space [17]. It is more convenient to use a set of coordinates with one (hyper-) radial variable and five dimensionless angles. The asymptotic play then runs on a graspable one-dimensional stage yet allowing mathematically correct three-body boundary conditions [18]. This set of so called hyperangular coordinates [19] is given as $\{\rho, \alpha_i, \frac{\mathbf{x}_i}{x_i}, \frac{\mathbf{y}_i}{y_i}\} \equiv \{\rho, \Omega_i\}$, where the hyperradius ρ and the hyperangles α_i are defined as

$$\rho = \sqrt{x_i^2 + y_i^2}, \quad \alpha_i = \arctan\left(\frac{x_i}{y_i}\right), \quad i = 1, 2, 3. \quad (192)$$

We shall from now on omit the index when any one of the three sets of coordinates is implied. The kinetic energy operator in these variables is

$$T = \frac{\hbar^2}{2m} \left(-\rho^{5/2} \frac{d^2}{d\rho^2} \rho^{5/2} + \frac{15/4}{\rho^2} \right) + \frac{\hbar^2}{2m\rho^2} \hat{\Lambda}^2, \quad (193)$$

$$\hat{\Lambda}^2 = -\frac{1}{\sin(2\alpha)} \frac{d^2}{d\alpha^2} \sin(2\alpha) - 4 + \frac{\hat{l}_x^2}{\sin^2 \alpha} + \frac{\hat{l}_y^2}{\cos^2 \alpha}. \quad (194)$$

The components of the total wavefunctions are now expanded in terms of hyperangular functions $\Phi_n(\rho, \Omega) = \sum_{i=1}^3 \Phi_n^{(i)}(\rho, \Omega_i)$

$$\Psi(\rho, \Omega) = \rho^{-5/2} \sum_n f_n(\rho) \Phi_n(\rho, \Omega). \quad (195)$$

The hyperangular functions for each ρ are chosen to be the eigenfunctions of the angular part of the Fadeev equations

$$\hat{\Lambda}^2 \Phi_n^{(i)} + \frac{2m\rho^2}{\hbar^2} V_i \Phi_n = \lambda_n(\rho) \Phi_n^{(i)}. \quad (196)$$

The radial functions $f_n(\rho)$ satisfy the coupled set of radial equations

$$\left(-\frac{d^2}{d\rho^2} + \frac{\lambda_n(\rho)}{\rho^2} + \frac{15/4}{\rho^2} - \frac{2mE}{\hbar^2} \right) f_n = \sum_{n'} \left(2P_{nn'} \frac{d}{d\rho} + Q_{nn'} \right) f_{n'},$$

$$P_{nn'}(\rho) = \int d\Omega \Phi_n(\rho, \Omega) \frac{d}{d\rho} \Phi_{n'}(\rho, \Omega), \quad Q_{nn'} = \int d\Omega \Phi_n(\rho, \Omega) \frac{d^2}{d\rho^2} \Phi_{n'}(\rho, \Omega). \quad (197)$$

For illustration we consider the case of three identical spin zero particles and s-waves only. The extension to higher orbital momenta, non-zero spins and different masses is straightforward but somewhat tedious.

We then write the hyperangular function as

$$\Phi_n(\rho, \Omega) = \sum_{i=1}^3 \frac{\phi_n(\rho, \alpha_i)}{\sin(2\alpha_i)}. \quad (198)$$

The three Fadeev equations are identical in this case. To write the equation explicitly in one of the Jacobi sets we have to “rotate” two other components into the chosen set. This rotation, which expresses one set of coordinates by another and subsequently integrates out the four angular variables of \mathbf{x} and \mathbf{y} is performed by an operator \hat{R} given for s-waves and identical particles can be easily found to be

$$\hat{R}\phi = \frac{2}{\sqrt{3}} \int_{|\pi/3-\alpha|}^{\pi/2-|\pi/6-\alpha|} d\alpha' \phi(\rho, \alpha'). \quad (199)$$

The angular part of the Fadeev equation is then

$$\left(-\frac{d^2}{d\alpha^2} - \tilde{\lambda} \right) \phi(\rho, \alpha) + \rho^2 v(\rho \sin \alpha) \left(\phi(\rho, \alpha) + \frac{4}{\sqrt{3}} \int_{|\pi/3-\alpha|}^{\pi/2-|\pi/6-\alpha|} d\alpha' \phi(\rho, \alpha') \right) = 0 \quad (200)$$

where $v(z) \equiv 2mV(\sqrt{2}z)/\hbar^2$ and $\tilde{\lambda} \equiv \lambda + 4$.

11.2 Asymptotic behavior of the angular eigenvalues

Let us now consider the asymptotic behavior of $\tilde{\lambda}$ for small and large ρ . For $\rho = 0$ the solution of Equation 200, which obeys the boundary conditions of being zero for both $\alpha = 0$ and $\pi/2$, is $\sin(2n\alpha)$ with an eigenvalue $\lambda_n = 4n^2$. This is in fact the hyperharmonic spectrum for the s-waves [19]. The eigenvalue $\tilde{\lambda}$ for small ρ is now obtained in first order perturbation theory as

$$\tilde{\lambda}_n = 4n^2 + 3v(0)\rho^2, \quad n = 1, 2, \dots \quad (201)$$

For large ρ we consider separately the cases corresponding to the bound and continuum states of the potential v .

For a bound state and for ρ much larger than the spatial extension of this state we can neglect the exponentially small integral term in the Equation 200. Introducing a new variable $z = \rho \sin \alpha$ one rewrites the equation as

$$\left(-\frac{d^2}{dz^2} - \frac{\tilde{\lambda}}{\rho^2} + v(z) \right) \phi = 0. \quad (202)$$

With the boundary condition $\phi(z=0) = \phi(z=\rho\pi/2 \rightarrow \infty) = 0$ this equation is equivalent to the two-body problem with the potential v . The two-body bound state with

the binding energy $\epsilon > 0$ and the radial function $u(z)$ gives the following angular eigenvalue and eigenfunction

$$\begin{aligned}\tilde{\lambda}_1 &= -\frac{2m\epsilon}{\hbar^2}\rho^2 + \int dz u(z) (u'(z)z + u''(z)z^2), \\ \phi_1(\rho, \alpha) &= \sqrt{\rho} u(\rho \sin \alpha), \\ Q_{11} &= -\frac{1}{4}\frac{1}{\rho^2} + \frac{1}{\rho^2} \int dz u(z) (u'(z)z + u''(z)z^2).\end{aligned}\quad (203)$$

The eigenvalue corresponding to a two-body bound state therefore diverges parabolically with ρ with a factor proportional to the two-body binding energy. Note that the second terms in the expressions for $\tilde{\lambda}$ and Q cancel when put in the radial equation. Thus the proper two-body radial asymptotics is restored which describes the motion of one of the particles against the bound system of the other two particles.

Now, we shall consider the case of a short range potential, that is the potential which can be neglected outside a finite range r_0 . The results, however, are valid for any potential which falls off faster than $1/r^2$ at large distances [18]. For $\rho \gg r_0$ Equation 200 reduces to first order in r_0/ρ to

$$\left(-\frac{d^2}{d\alpha^2} - \tilde{\lambda}(\rho)\right) \phi(\rho, \alpha) + \rho^2 v(\rho\alpha) \left(\phi(\rho, \alpha) + \alpha \frac{8}{\sqrt{3}} \phi(\rho, \pi/3)\right) = 0.$$

To solve this equation one divides the α -space into two regions I and II, where $\rho \sin \alpha$ is respectively more and less than r_0 . In region I, where $\alpha > r_0/\rho$, the potential is negligible and this equation becomes

$$\left(-\frac{d^2}{d\alpha^2} - \tilde{\lambda}\right) \phi^{(I)}(\rho, \alpha) = 0 \quad (204)$$

with the solution $\sin(\sqrt{\tilde{\lambda}}(\alpha - \pi/2))$ vanishing at $\pi/2$ independent of λ . In region II, where $\alpha < r_0/\rho$, one has instead the equation

$$\left(-\frac{d^2}{d(\rho\alpha)^2} + v(\rho\alpha)\right) \phi^{(II)}(\rho, \alpha) = -v(\rho\alpha) \alpha \frac{8}{\sqrt{3}} \phi^{(I)}(\rho, \pi/3), \quad (205)$$

where the small term λ/ρ^2 has been neglected. The total solution of Eq. 205, the homogeneous plus the inhomogeneous one, is now

$$\phi^{(II)}(\rho, \alpha) \propto u_0(\rho\alpha) - \alpha \frac{8}{\sqrt{3}} \phi^{(I)}(\rho, \pi/3), \quad (206)$$

where the homogeneous solution $u_0(\rho\alpha)$ is the wave function describing the state of zero energy in the potential v , which outside the range of the potential ($\rho\alpha > r_0$) has the form $\rho\alpha + a$, where a is the scattering length.

The eigenvalue equation for $\tilde{\lambda}$ now arises by matching of the derivative of the logarithm of the two solutions at the point $\alpha = r_0/\rho$. To first order in r_0/ρ one then immediately obtains

$$-\sqrt{\tilde{\lambda}} \cos(\sqrt{\tilde{\lambda}} \frac{\pi}{2}) + \frac{8}{\sqrt{3}} \sin(\sqrt{\tilde{\lambda}} \frac{\pi}{6}) = \frac{\rho}{a} \sin(\sqrt{\tilde{\lambda}} \frac{\pi}{2}) \left(1 + \lambda \frac{r_0}{\rho} \frac{r_0 + a}{\rho}\right). \quad (207)$$

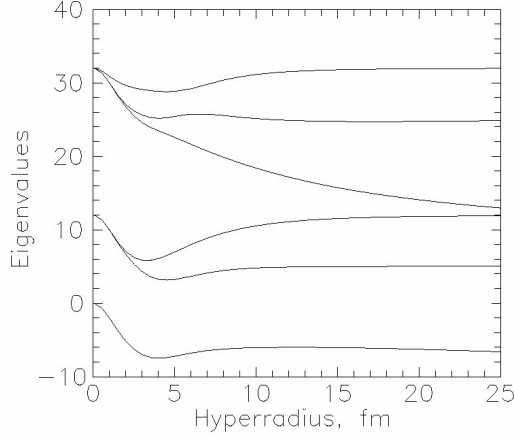


Figure 7 The six lowest lying angular eigenvalues λ as function of ρ for a neutron-core gaussian potential, strength $S_{cn} = 10.7$ MeV and range parameter 2.55 fm, corresponding to one slightly bound state of binding energy $B_{cn} = 40$ keV. The core mass is 9 times the nucleon mass.

Neglecting the first order term in r_0/ρ one gets the zero order equation of Efimov [11]. For finite $a \gg r_0$, the first two terms of λ in powers of a/ρ are

$$\begin{aligned} \tilde{\lambda}_n &= 4n^2 \left(1 - \frac{4}{\pi} \frac{3a}{\rho}\right), & \phi_n &= \frac{\sin(\sqrt{\tilde{\lambda}}(\alpha - \pi/2))}{\sqrt{\pi/4 - \sin(\sqrt{\tilde{\lambda}}\pi)/(4\sqrt{\tilde{\lambda}})}}, \quad n = 1, 2, \dots \\ P_{12} &= -P_{21} = \frac{a^3}{\rho^4} \frac{54}{\pi^3} (8\pi^2 - 3), & Q_{11} &= -\frac{a^2}{\rho^4} 6 \left(4 + \frac{3}{\pi^2}\right) \dots \end{aligned} \quad (208)$$

The mixing terms P and Q fall off as ρ^{-4} and therefore the radial equations are asymptotically decoupled thus allowing to impose mathematically correct boundary conditions in each of the coupled radial equations independently.

For finite scattering length $\tilde{\lambda}_n$ therefore return back to the hyperharmonic spectrum with the scattering length as a governing parameter.

For infinite scattering length ($a = \infty$) Eq. 207 has a solution $\tilde{\lambda}_\infty = -1.01251$, which substituted into the radial Eq. 197 implies that the equation asymptotically has an effective attractive potential given by $-1.26251/\rho^2$. Such a potential is known to produce the “falling towards the center” phenomenon [20] but when corrected at small ρ according to 201 instead results in an infinite number of bound states [15]. This anomaly is called the *Efimov effect*.

If only two of the three scattering lengths are infinitely large the effect still takes place. One infinite scattering lengths does not produce the effect as this gives too small asymptotic value for $\tilde{\lambda}$.

Let us consider now the Coulomb repulsion v_c which enters the angular equa-

tion as

$$\rho^2 v_c(\rho \sin \alpha) = \frac{\eta \rho}{\sin \alpha} \equiv \eta \rho + \eta \rho \frac{1 - \sin \alpha}{\sin \alpha}, \quad (209)$$

where $\eta = 2mZ^2e^2/\sqrt{2}\hbar^2$. The constant term can be included exactly while for the second we shall use the first order perturbation theory. The applicability of the perturbation theory is justified when the correction to the eigenvalue is small. The relative contribution of the second term is in our case 0.7 for the first continuum eigenfunction. This value although being not much less than unity still allows to trace the general trend. For the lowest continuum states we then have

$$\lambda_1(\rho) = 4 + \frac{16}{3\pi}\eta\rho, \quad \lambda_2(\rho) = 16 + \frac{704}{105\pi}\eta\rho, \dots \quad (210)$$

The Coulomb repulsion therefore leads to the eigenvalues which grow linearly with ρ . This dependence restores the $1/\rho$ repulsion in the radial equations. The Efimov effect can not take place in this case.

The results 203 for the bound state are unchanged since the only assumption made concerned the exponential fall off of the two-body radial function which is still valid in the presence of the Coulomb field.

11.3 Application to two-neutron halo

The neutron-neutron interaction is rather well known [21]. Since for loosely bound systems only the low energy properties of the potentials are important [18] and since the s-waves are the ones responsible for the Efimov effect, we shall use a simple attractive central potential of Gaussian form, which reproduces the measured s-state scattering length and effective range, i.e. $-31 \text{ MeV} \exp(-(r/1.8\text{fm})^2)$ [5]. The neutron-core potential can also be assumed to be gaussian, i.e. $-S_{cn} \exp(-(r/2.55\text{fm})^2)$ [5].

The neutron-core two-body system is first investigated as function of the strength S_{cn} . The scattering length is computed for each potential and the angular part of the three-body problem is solved. Eigenvalues $\lambda_n(\rho)$ and wavefunctions Φ_n are obtained for ρ -values up to 20 times the largest scattering length. The resulting lowest lying eigenvalues are shown in Fig. 7 as function of ρ for a neutron-core potential with one slightly bound state with the binding energy $B_{cn} = 40 \text{ keV}$. We recognize the hyperharmonic spectrum at $\rho = 0$, namely $\lambda = K(K + 4)$ where K is a non-negative even integer [19]. The odd integers are connected with odd parity. The convergence towards the same spectrum at $\rho = \infty$ is clearly seen for the curves number 3,4 and 6 (starting from bottom), whereas number 1, 2 and 5 have only just started to bend over, respectively towards the parabolic divergence, 0 and 32. The slow divergence of the lowest eigenvalue is the signature of a barely bound state in the neutron-core potential.

The radial Eqs. 197 are now solved and the resulting energies for the ground state and the first excited state are shown in Fig. 8 as function of S_{cn} . The two- and three-body systems are bound respectively for $S_{cn} > 9.510 \text{ MeV}$ or $S_{cn} > 6.6 \text{ MeV}$. Extremely close to the two-body threshold, but still below ($S_{cn} \approx 9.505 \text{ MeV}$), appears the first excited three-body state, where the neutron-core scattering length is

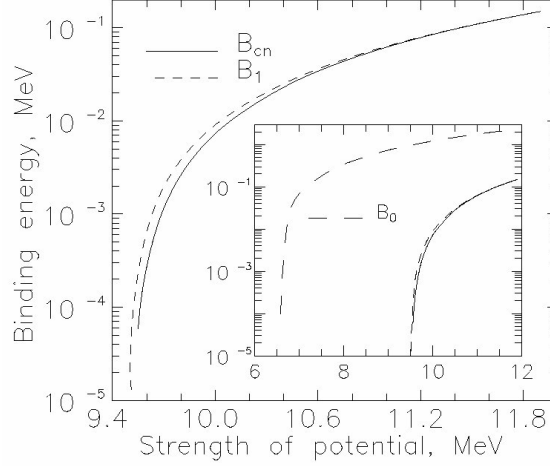


Figure 8 Binding energies of the two-body ground state (B_{cn} solid curve) and the first excited state (B_1 dashed curve) of the three-body system as functions of potential strength S_{cn} . The insert also includes the three-body ground state (B_0 long-dashed curve). The core mass is 9 times the nucleon mass.

about 18000 fm. Infinitely many bound states appear, one after the other, when S_{cn} is increased from 9.505 MeV to 9.510 MeV. The closer we are to the two-body threshold the larger is the number of bound states. This narrow region could be called the Efimov region.

The convergence of the λ -expansion in Eq. 195 is very fast for both ground and excited states. The lowest λ accounts for more than 99.9% of the norm of both wavefunctions and provides binding energies with an accuracy of about 2%. The binding energy of the first excited state increases until the state disappears into the two-body continuum at $S_{cn} \approx 11.9$ MeV, where the neutron-core scattering length is about -15 fm. Therefore the one-neutron separation energy for this state ($B_1 - B_{cn}$) will first increase and then decrease as the potential strength is increased. Note that the states preferentially occur for bound neutron-core systems. The ground state wavefunction is concentrated in the pocket region near 4 fm. The excited state has unlike the ground state a node in the radial wavefunction, which is peaked at ρ -values much larger than the ranges of the nuclear potentials. Consequently the ground state and the first excited state are orthogonal although they both have the same angular momentum quantum numbers.

The mean square hyperradius of the first excited state is shown in Fig. 9 as function of an energy, which is defined as the one- or two-body separation energy above and below the two-body threshold, respectively. Close to the three-body threshold the mean square radius should obey the three-body asymptotics, i.e. go as a logarithm of the three-body binding energy [22]. This occurs outside the range shown in the Fig. 9. When the binding energy increases towards about 2 keV, the mean square hyperradius decreases to about 10^4 fm². Then both turn around until the

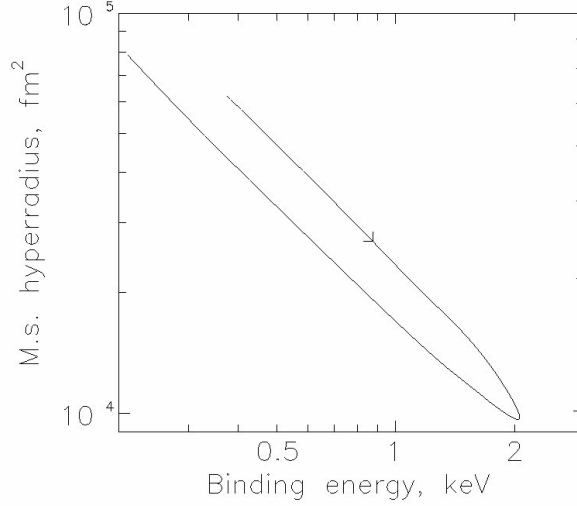


Figure 9 The mean square hyperradius $\langle \rho^2 \rangle$ of the three-body system as function of an energy defined as the one- or two-neutron separation energy above and below the two-body threshold, respectively. The arrow indicates the direction of increasing potential strength. The core mass is 9 times the nucleon mass.

excited three-body state disappears into the two-body continuum. The mean square radius has here reached the asymptotic region and scales inversely with energy [22].

We thus conclude that the two-neutron halo nuclei is a type of system where the Efimov effect might take place. The most promising candidate would be a system where a neutron is added to a weakly bound one neutron halo. For the most distinct case the scattering length in the neutron-core system should be about -20 fm corresponding to the neutron-core binding energy of ≈ 100 keV. The spatial extension of the first three-body excited state at this point is estimated to be about 100 fm with the binding energy about 2 keV.

More elaborate three-body calculations with spin-spin, spin-orbit, Pauli blocking and finite range interactions have also been performed. For a review, see Ref. [1]. A variational approach using an expansion on hyperspherical harmonics is one of the techniques used. In terms of the Jacobian coordinates and in a LS representation the total wavefunction of the three-body system is (for simplicity, we use again the notation of Fig. 6(b))

$$\Psi_{Jm}^T = \frac{1}{R^{5/2}} \sum \chi_{kl\rho\ell\lambda}^{\text{LS}}(R) \left\{ \mathcal{Y}_{KL}^{\ell\rho\ell\lambda}(\Omega_5) \otimes X_S \right\}_{JM} \cdot X_{TMT} \quad (211)$$

where the “hyper radius” R is defined as

$$R^2 = \rho^2 + \lambda^2.$$

It is a collective translationally, rotationally and permutation invariant variable. The “hyperharmonic” basis functions $\mathcal{Y}_{KL}^{\ell\rho\ell\lambda}(\Omega_5)$ are functions of 5 spherical

angles $\Omega_5 = (\alpha, \hat{\rho}, \hat{\lambda})$ containing the hyperangle $\alpha = \arctan(\rho/\lambda)$ which extracts part of the radial correlations. $X_S(1, 2)$ is the coupled two-nucleon spin function and likewise for isospin. The ‘‘hypermoment’’ K is connected with the principal quantum number, $K = \ell_\rho + \ell_\lambda + 2n$ ($n = 0, 1, 2, \dots$).

The hyperspherical harmonics have the explicit form

$$\mathcal{Y}_{KLM_L}^{\ell_\rho \ell_\lambda}(\Omega_5) = \phi_K^{\ell_\rho \ell_\lambda}(\alpha) \left\{ Y_{\ell_\rho}(\hat{\rho}) \otimes Y_{\ell_\lambda}(\hat{\lambda}) \right\}_{LM_L} \quad (212)$$

$$\phi_k^{\ell_\rho \ell_\lambda}(\alpha) = N_K^{\ell_\rho \ell_\lambda} (\sin \alpha)^{\ell_\rho} (\cos \alpha)^{\ell_\lambda} \cdot P_n^{\ell_\rho+1/2, \ell_\lambda+1/2}(\cos 2\alpha) \quad (213)$$

where $P_n^{\alpha, \beta}$ is the Jacobi polynomial, $N_K^{\ell_\rho \ell_\lambda}$ a normalization coefficient and $n = (K - \ell_\rho - \ell_\lambda)/2$.

When the expansion 211 is inserted in Eqs. 183, 184, with the definitions 185, a set of one-dimensional coupled differential equation in the variable R is obtained. These are solved numerically as explained in detail in Refs. [23, 24]. These calculations converge rapidly for the wave function but slowly for the eigenenergies, as we have seen in the last Section.

Another strict three-body approach is to solve the Fadeev equations. In coordinate-space the i -th wave function is given a bipolar angular momentum decomposition

$$\psi_{JM}^T(i) = \frac{1}{\rho\lambda} \sum \psi_{\ell_\rho \ell_\lambda}^{S_j \Sigma}(\rho, \lambda) \left\{ Y_{\ell_\lambda}(\hat{\lambda}) \otimes \left(\chi_k \otimes [Y_{\ell_\rho}(\hat{\rho}) \otimes X_{S_i}]_j \right)_\Sigma \right\}_{JM} \cdot X_{TM_T}. \quad (214)$$

When these expansion are inserted into the Fadeev equations a set of two-dimensional coupled differential equations are obtained and solved numerically [25].

The three-body calculations are very sensitive to the choice of the neutron-neutron and neutron-core interactions. Several authors have performed these calculations for ^{11}Li and ^6He (see Ref. [1], and references therein). With a consistent choice of potentials which reproduce known data for neighboring nuclei, the binding energies, resonant states, and rms radii are well reproduced within most approaches (even the simpler ones of the last two Sections).

Results concerning details which are not experimentally obtainable are sometimes controversial and not a good basis to distinguish if a model is better than another. As an example we cite the search for di-neutrons and cigar structures in three-body systems. This can be done, in principle, by looking at the probability of finding the neutrons in a position of interest. For convenience, let us introduce [34] the function

$$\Omega(R, r) = 8\pi R^2 r^2 \int_0^\pi |\psi|^2 \sin \theta d\theta \quad (215)$$

where $R = \lambda$, $r = \rho$, in terms of the Jacobian coordinates for a very heavy (recoil neglected) core. ψ is the wavefunction of the system and θ in the angle between \mathbf{R} and \mathbf{r} . Integration over the spin coordinates are implicit. In Refs. [26] and [27] two peaks in the contour plot of $\Omega(R, r)$ were obtained. One could argue if they represent

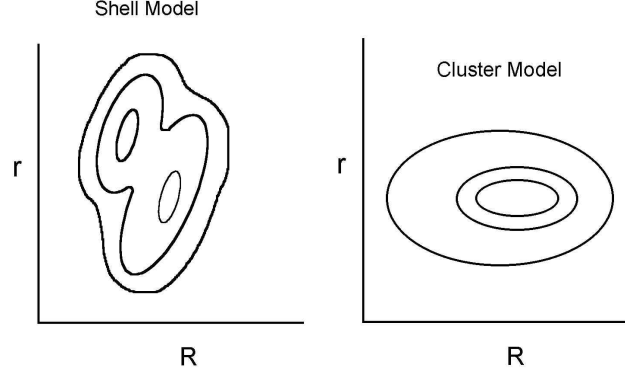


Figure 10 Density contour plots for the valence neutrons in ${}^8\text{He}$ in shell model and cluster model.

two geometrical conformations, the cluster ${}^4\text{He} + 2n$ dineutron structure and a cigar-shaped structure with two neutrons on the opposite side of ${}^4\text{He}$. However, as claimed by T. Suzuki [34] these two peaks do not necessarily mean the existence of such configurations, especially the cigar-structure. For example, if the wavefunction of the two-neutrons is taken as a product of two $p_{3/2}$ -harmonic oscillator wavefunction of a shell-model with size parameter a :

$$\begin{aligned} \Omega(R, r) = & \frac{16}{9\pi a^2} \left(\frac{8}{5}\right)^5 \left(\frac{rR}{2a^2}\right)^2 \left[\left(\frac{R}{a}\right)^4 + \left(\frac{r}{2a}\right)^4 - \frac{4}{3} \left(\frac{rR}{2a^2}\right)^2 \right] \\ & \times \exp \left[-\frac{8}{5} \left\{ \left(\frac{R}{a}\right)^2 + \left(\frac{r}{2a}\right)^2 \right\} \right]. \end{aligned} \quad (216)$$

This function has a reflection symmetry $\Omega(R, r) = \Omega(r/2, 2R)$ so that two peaks naturally appear as displayed in left-side of Fig. 10. If the wavefunction ψ is given by a cluster configuration, one obtains a single peak in the plot of $\Omega(R, r)$ as schematically shown in right-side of Fig. 10. Thus, while a dineutron configuration can be easily identified, other kind of structures (like cigars) may be not.

Questions like the existence of a dineutron structure in ${}^{11}\text{Li}$ or ${}^6\text{He}$ are not easily solved by three-body calculations. They depend on the technique, choice of potentials, etc. used in these models. To be more specific about the structure of such nuclei these models have to be tested by experiments looking for additional variables other than the binding energies and rms radii, only.

12 References

1. M.V. Zhukov, B.V. Danilin, D.V. Fedorov, J.M. Bang, I.J. Thompson and J.S. Vaagen, Phys. Rep. **231** (1993) 231.
2. G.L. Squires and A.T. Stewart, Proc. Roy. Soc. (London) **A230** (1955) 19.

3. A.B. Migdal, Sov. J. Nucl. Phys. **16** (1973) 238.
4. L.M. Delves, Adv. Nucl. Phys. **5** (1972) 1.
5. L. Johannsen, A.S. Jensen and P.G. Hansen, Phys. Lett. **B244** (1990) 357.
6. G.F. Bertsch and H. Esbensen, Ann. of Phys. **209** (1991) 327.
7. A. Bohr and B.R. Mottelson, “*Nuclear Structure*”, Vol. I, Benjamin, New York, 1969.
8. R. Reid, Ann. Phys. (N.Y.) **50** (1968) 411.
9. G. Bertsch and S.F. Tsai, Phys. Rep. **18** (1975) 127.
10. P.G. Hansen and B. Jonson, Europhys. Lett. **4** (1987) 409.
11. V. Efimov, Phys. Lett., **B33** (1970) 563; Sov. Jour. Nucl. Phys. **12** (1971) 589.
12. V. Efimov, Nucl. Phys. **A210** (1973) 157.
13. C.A. Bertulani, L.F. Canto and M.S. Hussein, Phys. Rep. **226** (1993) 281.
14. V.N. Efimov, Comm. Nucl. Part. Phys. **19** (1990) 271.
15. D.V. Fedorov and A.S. Jensen, Phys. Rev. Lett. **71** (1993) 4103.
16. P.G. Hansen, Nucl. Phys. **A553** (1993) 89c.
17. S.P. Merkuriev, Sov. J. Nucl. Phys. **19** (1974) 222.
18. D.V. Fedorov, A.S. Jensen and K. Riisager, Phys. Rev. **C49** (1994) 201; **C50** (1994) 2372.
19. R.I. Jibuti and N.B. Krupennikova, The Hyperspherical Functions Method in few-body quantum mechanics, Mecniereba, Tbilisi, 1984 (in Russian).
20. L.D. Landau and E.M. Lifshitz, “*Quantum Mechanics – Non-relativistic Theory*”, Pergamon Press, 1975.
21. O. Dumbrajs et al., Nucl. Phys. **B216** (1983) 277.
22. D.V. Fedorov, A.S. Jensen and K. Riisager, Phys. Lett. **B312** (1993) 1; Phys. Rev. **C49** (1994) 201.
23. B.V. Danilin, M.V. Zhukov, A.A. Korshennikov, L.V. Chulkov and V.D. 'Efros, Sov. Jour. Nucl. Phys. **49** (1989) 351.
24. B.V. Danilin, M.V. Zhukov, A.A. Korshennikov and L.V. Chulkov, Sov. Jour. Nucl. Phys. **53** (1991) 71.
25. J.M. Bang and I.J. Thompson, Phys. Lett. **B279** (1992) 201.
26. V.I. Kukulin, V.M. Krasnopol'sky, V.T. Voronchev and P.B. Suzanov, Nucl. Phys. **A453** (1986) 365.
27. B.V. Danilin, M.V. Zhukov, A.A. Korshennikov V.D.'Efros and L.V. Chulkov, Sov. Jour. Nucl. Phys. **48** (1988) 766.
28. W. Glöckle, in “*Computational Nuclear Physics I*”, K. Langanke, J.A. Maruhn and S.E. Koonin, eds., Springer, Berlin, 1991.
29. M. Fabre de la Ripelle, Lecture Notes in Physics **273** (1987) 283.
30. R.B. Wiringa, Few-Body Systems Suppl. **1** (1986) 130.
31. L.D. Fadeev, “*Mathematical aspects of the three-body problem in the quantum scattering theory*” (Steklov Mathematical Institute, Leningrad, 1963) [English translation: Israel Program for Scientific Translation, Jerusalem, 1965].
32. W. Glöckle, “*The quantum mechanical few-body problem*”, Springer, Berlin, 1983.
33. K.E. Schmidt, Lectures Notes in Physics **273** (1987) 363.

34. Y. Suzuki, Nucl. Phys. **A528** (1991) 395.